MASTERARBEIT | MASTER'S THESIS

Titel | Title

Chemogenetic modulation of the dorsal raphe: Enhancing motor recovery after ischemic stroke in a photothrombotic mouse model

verfasst von | submitted by

Livia Noelle Wieland BSc

angestrebter akademischer Grad | in partial fulfilment of the requirements for the degree of

Master of Science (MSc)

Wien | Vienna, 2024

Studienkennzahl lt. Studienblatt | Degree programme code as it appears on the student record sheet:	UA 066 606
Studienrichtung lt. Studienblatt | Degree programme as it appears on the student record sheet:	Masterstudium Drug Discovery and Development
Betreut von | Supervisor:	Ass.-Prof. Marietta Zille BSc MSc PhD

Acknowledgements

First and foremost, I would like to express my deepest gratitude to Ass.-Prof. Marietta Zille, BSc MSc PhD and Prof. Dr. med. Christoph Harms for their outstanding guidance and support throughout this project. Their expertise and invaluable advice continually motivated me to push forward, allowing me to grow both academically and personally.

I would like to express my gratitude to Dr. med. Leif Koschützke for his constant support in the lab, always taking the time to guide and assist me throughout the project. I would also like to extend my sincere thanks to Dr. med. Christian Hoffmann, whose invaluable guidance in scientific writing was instrumental in shaping and refining my thesis. The generous sharing of their expertise provided me with invaluable learning opportunities, for which I am deeply grateful.

A heartfelt thank you goes to Amido Daugardt, with whom I had the pleasure to collaborate closely and join forces on this project. His tremendous support and the wealth of knowledge he shared with me in the lab made this journey not only successful but also truly enjoyable and memorable.

Additionally, I am deeply grateful for the entire lab team, especially Hannes Diestelmeier, Polina Bugaeva, and Sylwia Piatek, whose creation of an exceptionally positive atmosphere in the lab has been an immense source of support and motivation from the very beginning.

I would also like to express my heartfelt thanks to all my friends, whether long-time friends from my hometown Mutlangen, those who became an important part of my life during my early adult years in Vienna, or the friends I have made in Berlin, who have quickly found a special place in my heart. Without their support, I wouldn’t be where I am today. I am endlessly grateful for their encouragement in every step of my journey.

Finally, I would like to thank my entire family, with a special thanks to my parents Yvonne Bonnet-Wieland and Klaus Wieland, who made all this possible in the first place. They have always supported me, not only throughout my studies but in every aspect of my life.

Content

List of figures

List of tables

Abstract

Stroke is one of the primary causes for mortality and disability globally, with motor impairments being among the most common and debilitating consequences. Motor recovery after stroke is often limited, with many patients remaining dependent on assistance despite rehabilitative efforts. Neuroplasticity plays a crucial role in post-stroke recovery, with the brain reorganizing itself to compensate for lost function. Recent research suggests that serotonin plays a key role in neuroplasticity, and the dorsal raphe nucleus (DRN), with its extensive serotonergic projections, may be crucial in modulating these neuroplastic processes.

This study aimed to investigate whether targeted modulation of serotonergic transmission in the DRN can enhance motor recovery following a stroke in a photothrombotic mouse model. We hypothesized that increasing serotonergic transmission from the DRN would promote cortical neuroplasticity, facilitating improved motor recovery. To test this hypothesis, we developed a chemogenetic mouse model to selectively activate DRN serotonergic neurons using Designer Receptors Exclusively Activated by Designer Drugs (DREADDs) and validated its effectiveness through cFOS activation in the DRN and DRN-related behavioral assessments in the elevated plus maze and open field test.

Our findings demonstrated that activating DRN serotonergic transmission using the hM3Dq DREADD promoted motor recovery, particularly in tasks requiring coordination and skilled walking. This suggests that enhancing serotonergic activity in the DRN facilitates the reorganization of motor networks, potentially by promoting neuroplasticity. Our chemogenetic approach offers a valuable model for investigating the role of serotonin in stroke recovery and may also have applications in studying other disease models beyond stroke rehabilitation. Insights from this study may pave the way for more targeted neuromodulatory treatments that can improve functional outcomes for stroke patients.

Abstrakt

Schlaganfall ist eine der Hauptursachen für Mortalität und Behinderung weltweit, wobei motorische Beeinträchtigungen zu den häufigsten und belastendsten Folgen gehören. Die Wiederherstellung motorischer Funktionen ist nach einem Schlaganfall oft begrenzt, und viele Patienten bleiben trotz rehabilitativer Maßnahmen auf Unterstützung angewiesen. Neuroplastizität spielt dabei eine entscheidende Rolle, da das Gehirn sich neu organisiert, um den Funktionsverlust zu kompensieren. Jüngste Forschungen deuten darauf hin, dass Serotonin eine Schlüsselrolle bei der Neuroplastizität spielt und der dorsale Raphe-Kern (DRN) mit seinen umfangreichen serotonergen Projektionen entscheidend zur Modulation dieser neuroplastischen Prozesse beitragen könnte.

Diese vorliegende Studie zielte darauf ab, zu untersuchen, ob die gezielte Modulation der serotonergen Übertragung im DRN die Wiederherstellung motorischer Funktionen nach einem Schlaganfall in einem photothrombotischen Mausmodell verbessern kann. Wir stellten die Hypothese auf, dass eine Erhöhung der serotonergen Übertragung vom DRN die kortikale Neuroplastizität fördert und dadurch und dadurch die Wiederherstellung motorischer Funktionen erleichtert. Um diese Hypothese zu testen, entwickelten wir ein chemogenetisches Mausmodell zur selektiven Aktivierung serotonerger Neuronen im DRN mittels Designerrezeptoren (DREADDs: Designer Receptors Exclusively Activated by Designer Drugs), die ausschließlich durch Designerdrogen aktiviert werden, und validierten dessen Wirksamkeit durch cFOS-Aktivierung im DRN sowie DRN-assoziierte Verhaltensbewertungen im Elevated-Plus-Maze- und Open-Field-Test.

Unsere Ergebnisse zeigten, dass die Aktivierung der serotonergen Übertragung im DRN mittels des hM3Dq Designerrezeptors die Wiederherstellung motorischer Funktionen, insbesondere bei Aufgaben, die Koordination und Geschicklichkeit erfordern, förderte. Dies deutet darauf hin, dass die Verstärkung der serotonergen Aktivität im DRN die Reorganisation motorischer Netzwerke erleichtert, möglicherweise durch Förderung der Neuroplastizität. Unser chemogenetischer Ansatz bietet ein wertvolles Modell zur Untersuchung der Rolle von Serotonin bei der Schlaganfall-Rehabilitation und könnte auch Anwendungen in anderen Krankheitsmodellen finden. Erkenntnisse aus dieser Studie könnten den Weg für

gezieltere neuromodulatorische Behandlungen ebnen, die die Wiederherstellung motorischer Funktionen für Schlaganfallpatienten verbessern könnten.

List of abbreviations

AAV	Adeno-associated virus
CNO	Clozapine N-oxide
DRN	Dorsal raphe nucleus
EPM	Elevated plus maze
NDS	Normal donkey serum
SSRI	Selective serotonin reuptake inhibitor
tPA	Tissue plasminogen activator
TPH	Tryptophan hydroxylase
5-HT	5-Hydroxytryptamin

1 Introduction

1.1 Pathophysiology of ischemic stroke

Stroke affects approximately 13.7 million people and about 5.5 million people die annually due to stroke, thereby being the second most frequent cause of death and the leading cause for disability in the world. A stroke is a neurological condition caused by of blood flow interruption in the brain (Kuriakose & Xiao, 2020). In 2019, ischemic strokes made up approximately 62.4% of all strokes (Feigin et al., 2021).

The primary injury in ischemic stroke is caused by a lack of blood supply to the brain tissue, which causes a reversible loss of tissue function. If the blood flow is not restored in time, this reversible loss of function progresses to infarction, characterized by an irreversible damage of neurons. The lack of blood supply triggers a series of events, starting with the loss of electrical function in the neurons and advances to membrane dysfunction (Feske, 2021). This dysfunction causes an excessive influx of calcium into the cells, leading to the overactivation of neurons, exacerbating cellular damage. Additionally, ischemia generates reactive oxygen species, which cause oxidative stress and further harm cellular components such as proteins, lipids, and DNA. This cascade ultimately results in the destruction of cell membranes, contributing to the expansion of the infarcted area (Feske, 2021).

Based on the degree of reduction in blood flow, the ischemic region is categorized into the infarct core and the surrounding ischemic penumbra. In the core of the stroke, cell death occurs within minutes. In the ischemic penumbra, collateral blood flow provides sufficient circulation to delay the onset of infarction, which can range from minutes to several hours. This creates an opportunity for immediate treatment to restore blood flow and minimize the extent of the lesion (Teasell et al., 2005).

1.2 Stroke treatment

1.2.1 Acute treatment

The primary objectives of acute treatments are to rapidly restore normal cerebral blood flow and to protect neurons in the penumbra from being irreversibly damaged (Brott Thomas & Bogousslavsky Julien, 2000). This is either done by intravenous thrombolysis or mechanical thrombectomy. In intravenous thrombolysis, recombinant tissue plasminogen activator (tPA) is administered intravenously to induce fibrinolysis.

This treatment is effective if administered within a 4.5-hour window from symptom onset (Phipps & Cronin, 2020). Mechanical thrombectomy, where the thrombus is removed via a stent retriever, can be effective even after 24 h of symptom onset, if there is still penumbral tissue detectable using specialized imaging (Phipps & Cronin, 2020). Especially those patients with large vessel occlusion such as of the middle cerebral artery or the internal carotid artery can benefit rather from mechanical thrombectomy than from intravenous thrombolysis (Feske, 2021). Reperfusion strategies early after stroke onset can salvage the tissue at risk and thereby limit infarct size and neurological deficits. However, only about 20 % of stroke patients receive an acute stroke treatment due to the short time-window for treatment or contraindications. For the remaining 80 % of stroke patients, no specific treatment is available yet.

1.2.2 Rehabilitation therapy

Stroke survivors often experience both, immediate and long-term disabilities. Common impairments after a stroke include motor, speech and language, swallowing, vision, sensation, and cognitive impairments, with motor impairment being most prevalent (Jiang et al., 2013). Up to now, rehabilitation therapy, which can involve physical, occupational, speech, and cognitive therapy, is the only option to restore lost functions (Kuriakose & Xiao, 2020). A great portion of stroke rehabilitation efforts is dedicated to restoring impaired body movements. For example, motor recovery through rehabilitation is based on the principle that motor learning promotes neuroplasticity, leading to increased dendritic sprouting and synaptogenesis. Despite physical therapy, functional recovery remains limited in many cases, highlighting the need for further treatment strategies to enhance motor recovery after stroke.

1.3 Neurological reorganization and motor recovery

A stroke lesion leads to the abrupt loss of numerous neurons and their synaptic connections (Teasell et al., 2005). To compensate this loss and restore lost function, a functional and structural reorganization of the brain happens weeks to months after stroke onset and differs across patients depending on the location and severity of the lesion (Jiang et al., 2013).

For this reorganization, a critical period with enhanced neuroplasticity opens, which resembles plasticity mechanisms during brain development (Murphy & Corbett, 2009). It was shown that the expression of genes and proteins relevant for neuronal growth, formation of new synapses and dendritic spine proliferation are increased and that

most recovery occurs within this time window (Murphy & Corbett, 2009). In particular, motor recovery is primarily linked to cortical plasticity and reorganization during the early stages of recovery (Li, 2017).

In animal models, recovery after injury in the motor cortex is associated with dendritic growth, axonal sprouting and synaptogenesis in areas surrounding the lesion but also in areas of the unaffected hemisphere that have functional connection to the injury site (Hermann & Chopp, 2012). Small strokes lead to more effective reorganization in adjacent areas within the affected hemisphere, while larger strokes involve broader, less effective reorganization in the unaffected hemisphere, resulting in diminished recovery (Teasell et al., 2005).

1.4 Influence of serotonin on neuroplasticity in motor recovery

Serotonin is an important neuromodulator involved in various physiological functions. It plays a crucial role in various forms of neuroplasticity, including sprouting, synaptogenesis, and neurogenesis (Michelsen et al., 2008). Serotonin further stimulates brain-derived neurotrophic factor expression (Martinowich & Lu, 2008), which supports cell survival, synaptic plasticity, and neurogenesis (Michelsen et al., 2008) and was shown to enhance motor recovery after stroke in rats (Cohen-Cory et al., 2010).

Due to the unmet need of treatment strategies to improve motor recovery after stroke despite physical therapy, numerous research groups have investigated selective serotonin reuptake inhibitors (SSRIs) as a therapeutic option, which elevate serotonin levels and are approved as antidepressant medications. It is suggested that the acute administration of SSRIs following ischemic stroke shifts the balance of excitatory and inhibitory signaling in the tissue surrounding the lesion, reactivating a form of plasticity similar to that observed during critical developmental periods. This shift is partially mediated by increased levels of brain-derived neurotrophic factor (Schneider et al., 2021).

Ng et al. (2015) suggest that fluoxetine can prolong the window for significant recovery after stroke by enhancing neuroplasticity. Their study demonstrated that while early motor training leads to significant recovery, fluoxetine facilitated complete recovery even when training was delayed, whereas those treated with saline did not achieve similar recovery. This indicates that fluoxetine may help maintain the brain's

responsiveness to rehabilitation by promoting plasticity, allowing for more effective motor recovery beyond the immediate post-stroke period.

Clinical studies investigating the effects of SSRIs after ischemic stroke showed mixed results. The FLAME trial demonstrated that early administration of fluoxetine, combined with physiotherapy, significantly enhanced motor recovery in ischemic stroke patients and moderate or severe motor deficits over a 3-month period, as measured by improvements on the Fugl-Meyer motor scale. However, the FOCUS trial found that fluoxetine 20 mg daily over the course of 6 months after acute stroke did not improve functional outcomes compared to placebo, as measured by the modified Rankin Scale. It may be that SSRIs need to be combined with rehabilitation to be effective, since in the FLAME study, all patients received rehabilitation therapy, whereas the FOCUS trial did not require rehabilitation therapy participation. However, the mixed results highlight the complexity of globally increasing serotonin levels, emphasizing that targeted modulation of serotonergic circuits may be more effective.

1.5 Dorsal raphe nucleus (DRN)

1.5.1 Structure and function

The raphe nuclei are located in the brainstem and are primarily composed of serotonergic neurons (Hornung, 2003). They can be further subdivided into the rostral raphe in the rostral pons and midbrain, and the caudal raphe in the caudal pons and medulla, which both can be distinguished based on their projections. The rostral raphe nuclei send projections to other brainstem nuclei and the spinal cord, and it can be further subdivided into the caudal linear nucleus, dorsal raphe, and median raphe nuclei (Hornung, 2003).

The dorsal raphe nucleus (DRN), which is located in the brainstem as highlighted in **Figure 1**, contains the largest group of serotonergic neurons of all serotonergic nuclei (Bacqué-Cazenave et al., 2020). The DRN serotonergic neurons show highly diverse projection targets and thereby regulate various behavioral responses and cognitive states, such as mood, anxiety, sensory and motor processes. Besides serotonin, the DRN also contains other neurotransmitters such as GABA, substance P, and very few neurons also produce catecholamines and neuropeptides like dynorphin, angiotensin, and enkephalin, contributing to the complexity of neurotransmission in this region (Ren et al., 2018).

The DRN projects primarily to the cerebral cortex, hippocampus, hypothalamus, and amygdala and can be subdivided based on the projection targets of its serotonin neurons. Serotonin neurons projecting to cortical and subcortical regions have a different cell distribution within the DRN. Neurons in the dorsal part of the mouse DRN primarily project to subcortical regions, while those in the ventral DRN project to the olfactory bulb and cortical areas (Ren et al., 2018). Commons (2015) showed that the caudal part of the DRN is involved in regulating hippocampal activity, while the rostral part is involved in networks regulating motor function and motivated behavior. Huang et al. (2019) identified five distinct serotonergic neuron subtypes that differ in their transcriptomic profiles and are divided into different areas of the DRN. However, the spatial organization of these serotonergic neuron subtypes did not align with the anatomical subdivisions based on their axonal projection targets. Okaty et al. (2020) further discovered that DRN serotonergic neurons consist of up to fourteen distinct molecularly defined subtypes.

Studies investigating the effect of DRN serotonergic transmission on brain networks show that the DRN plays a crucial role in modulating brain activity through its widespread serotonergic projections. For example, Grandjean et al. (2019) demonstrated that optogenetic activation of the DRN under anesthesia led to a decrease in brain activity, particularly in regions such as the motor cortex. This finding suggests that DRN activation can have inhibitory effects on motor-related areas in certain conditions. However, Hamada et al. (2024) observed increased brain activity during DRN activation in awake mice. This highlights the complexity of DRN function and suggests that its influence on brain activity may depend on the behavioral or conscious state of the organism. These opposing findings underline the need for further research to clarify the exact role of the DRN in modulating neural networks, particularly those related to motor control and recovery.

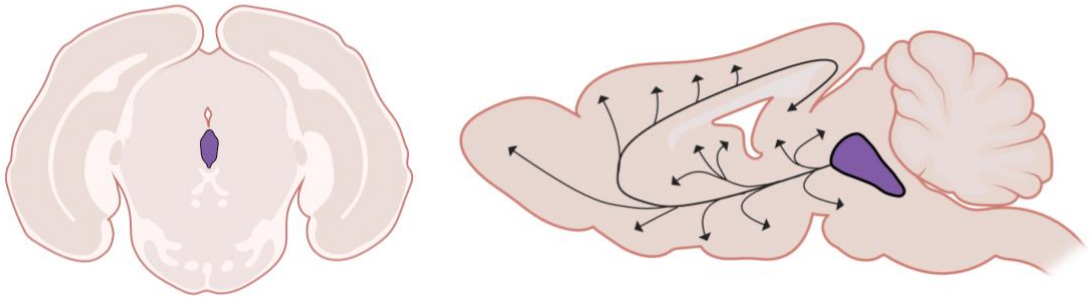

Figure 1. Anatomical localization of the DRN highlighted in purple. Coronal (left) and sagittal (right) view with projections. Created with BioRender.com.

1.5.2 DRN and behavior

Multiple studies explored the role of DRN serotonergic neurons in regulating behavior. Sena et al. (2003) investigated the role of DRN activity in anxiety behavior in rats, showing that increasing serotonergic activity through injecting the benzodiazepine inverse agonist FG 7142 into the DRN elevated anxiety-related responses in the elevated T-maze. They also demonstrated that lesions in the DRN induced by 5,7-dihydroxytryptamine hydrochloride produced anxiolytic effects. Ren et al. (2018) advanced the understanding of DRN serotonergic neurons by differentiating their role in anxiety-related behavior and locomotor activity based on their projection targets. They observed that DRN serotonergic neurons projecting to the orbitofrontal cortex decreased anxiety-related behavior, while those projecting to the central amygdala increased anxiety-related behavior. They also showed that both serotonergic subtypes reduced locomotion in the open field. This underscores the complexity of the different regions within the DRN, as well as their distinct functions and sometimes opposing influences on behavior.

2 Aims and experimental strategy

Despite acute treatments and rehabilitation after stroke, many individuals are not able to fully restore motor function and remain dependent on assistance in completing daily tasks.

Therefore, this research project aims to investigate whether targeted modulation of serotonergic transmission specifically in the DRN enhances neuroplasticity and thereby facilitates motor recovery after stroke. Our hypothesis is that increased serotonergic transmission from the DRN improves the efficacy of motor recovery by promoting neuroplasticity in the cortex.

To investigate this, we employed the photothrombotic mouse model of ischemic stroke, enabling precise targeting of the motor cortex with high reproducibility to investigate post-stroke motor recovery. We determined lesion volume and localization using magnetic resonance imaging (MRI) 24 hours after ischemia.

An experimental strategy to modulate DRN serotonergic transmission is by chemogenetics using Designer Receptors Exclusively Activated by Designer Drugs (DREADDs) as shown in **Figure 2**. These engineered receptors, delivered via Adeno-Associated Viruses (AAVs), are activated by a biologically inert synthetic ligand, such as Clozapine-N-Oxide (CNO), allowing to modulate neuronal activity spatially and temporally. This method provides a powerful tool to investigate the role of DRN serotonergic transmission in short and long-term motor recovery (Sternson & Roth, 2014).

We use two different DREADDs: the hM3Dq receptor for activating DRN serotonergic transmission by stimulating G_q signaling and the hM4Di receptor for inhibiting DRN serotonergic transmission by activating G_i signaling (Roth, 2016). Both receptor types are mutated G-protein-coupled muscarinic receptors that lost the affinity for the natural ligand acetylcholine but gained affinity for CNO (Zhu et al., 2016). It is suggested that CNO is metabolized into clozapine, an antipsychotic drug that may cause side effects by binding to additional receptors beyond the intended target. However, when administered in dosages between 0.1 and 3 mg/kg body weight (BW), CNO appears to be pharmacologically and behaviorally inert in mice. CNO rapidly distributes,

penetrates the central nervous system and remains present *in vivo* for at least 60 minutes after intraperitoneal injection (Roth, 2016).

In our experiment, we use the Cre-loxP system to achieve spatial control, specifically targeting serotonergic neurons. We deliver two AAVs: one encoding Cre recombinase under the control of the Tryptophan hydroxylase 2 (TPH2) promoter, ensuring expression only in serotonergic neurons, as TPH2 is the rate-limiting enzyme in the serotonin synthesis and only expressed in serotonergic neurons in the mouse central nervous system (Okaty et al., 2019), and the other AAV carrying either the DREADDs or EGFP under the neuron-specific human synapsin promoter. By using stereotactic injection, we restrict DREADD or EGFP expression to serotonergic neurons located in the DRN. By utilizing this chemogenetic system, we precisely modulate DRN serotonergic transmission with temporal control through the administration of CNO. This approach allows us to selectively activate or inhibit serotonergic neurons within the DRN at specific times, ensuring both spatial and temporal precision in modulating neuronal activity.

At the end of the experiment, we analyzed the DRN by immunohistochemistry. The expression of DREADDs or EGFP was confirmed and visually assessed for co-localization with 5-Hydroxytryptamin (5-HT). cFOS was visualized to quantify and investigate neuronal activity, as it is an early immediate gene expressed rapidly in response to neuronal activation (Chung, 2015). This allowed us to assess the number of active neurons following CNO administration, as CNO was administered 45 minutes before perfusion, providing insight into the effects of neuromodulation.

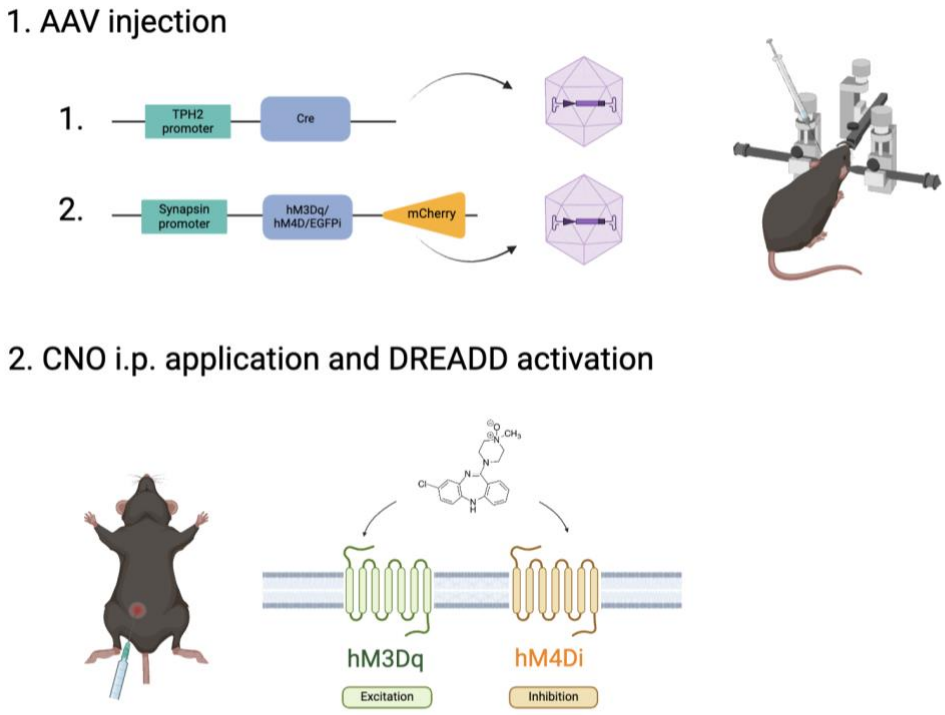

Figure 2. Chemogenetic modulation of DRN serotonergic transmission. AAV = adeno-associated virus, CNO = Clozapine N-oxide, DREADD = designer receptor exclusively activated by designer drugs, DRN = dorsal raphe nucleus**.** Created with BioRender.com

3 Materials and Methods

3.1 Materials

Table 1: Drugs.

Name	Company	Reference Number
Carprofen (Caprosol)	CP Pharma	114
Isofluran CP	CP Pharma	1214
Ketamine	CP Pharma	1203
Xylazine- hydrochloride (Xylavet 2 %)	CP Pharma	1206
Clozapine-N-oxide (CNO)	Enzo life sciences	BML-NS105-0025
Bupivacain	Charite central pharmacy	n.a.
Dexpanthenol eye ointment	Charite central pharmacy	n.a.

Table 2: Viral Vectors.

Name	Company	Reference Number
rAAV-Tph2-Cre (serotype AAV2/9)	Biohippo	BC-0309/PT-0396
pAAVhSyn-DIO- hM3D(Gq)-mCherry	Addgene	44361-AAV9
AAV9-hSyn-DIO-hM4d(Gi)-mCherry	Addgene	44362
pAAV-hSyn-DIO-EGFP	Addgene	50457

Table 3: Chemicals and Reagents

Name	Company	Reference Number
1x phosphate-buffered saline (PBS)	Thermo Fisher Gibco	10010023
Sodium azide	Sigma-Aldrich	S2002
Sodium chloride 0.9 %	Charite central pharmacy	n.a.
PFA 4%	ROTI Histofix	P087.2
Rose Bengal	Sigma-Aldrich	330000-5G
20 mg sucrose pellets	TestDiet	0030125150
Laboratory Chow	Ssniff	V1535-000
Normal Donkey Serum (NDS)	Sigma Aldrich	566460
Triton X-100	Sigma Aldrich	102533092
Bedding material	SAFE	304 34
Enrichment material	Thermofisher	n.a.
DAPI	Thermo Scientific	62248

Table 4: Primary antibodies

Name	Company	Reference Number	Validation
Anti-cFOS rabbit polyclonal	SynapticSystems	Cat #226008 RRID #AB_2891278	(Ollivier et al., 2024)
Anti 5-HT goat polyclonal	LS Bio	Cat #LS-C75755 RRID: n.a.	n.a.

Table 5: Secondary antibodies

Name	Company	Reference Number
Donkey anti-rabbit Alexa 488	Jackson Immunoresearch	Cat: 711-545-152 RRID: AB_2313584
Donkey anti-rabbit IgG (H+L) Highly Cross-Adsorbed Secondary Antibody, Alexa Fluor 546	Invitrogen	Cat: A10040 RRID: AB_2534016
Donkey anti-goat IgG (H+L) Highly Cross- Adsorbed Secondary Antibody, Alexa Fluor Plus 647	Invitrogen	A32849TR RRID: AB_2866498

Table 6: Instruments

Name	Company	Reference Number
Transponder Reader System	BMDS	DAS-8027 IUS
Transponders (Implantable RFID microchips)	BMDS	IPTT-300
Precision drill	Proxxon	28707
Masterflex Ismatec Reglo pump	Avantor	SERW2610.7100.01
Stereotactic frame	Kopf instruments	n.a.
Mini-centrifuge ROTILABO	Roth	T464.1
Vibratome	Leica VT 1000s	
TC-1000 temperature controller	CWE, Inc.	2221286P
Spinning disc confocal high content imaging microscope, Opera Phenix	Perkin Elmer	n.a.
Open field arena	Charite technical department	n.a.
Irregular ladder rung apparatus	Charite technical department	n.a.
Light source KL1500LCD, 150 W, 3000 K	Olympus	n.a.
7T magnetic resonance Scanner	Bruker PharmaScan 70/16 US	n.a.
ACE GigE high-speed cameras	Basler AG	209816
Elevated plus maze apparatus	Charite technical department	n.a.
Pneumatic Drug Injection System (PDES-02DX)	NPI Electronic GmbH	0210050
GoPro Hero12 Black	GoPro	n.a.
Suture material 5-0	Ethicon	V2130H

Table 7: Software

Name	Version	RRID
Fiji/ImageJ	2.14.0	SCR_002285
AnyMaze	7.1.6	SCR_014289
DeepLabCut	2.1.5	SCR_021391
R analysis software	4.4.0	SCR_001905
ANALYZE	5.0	SCR_005988
MATLAB		SCR_001622
Prism	10.3.0	SCR_002798

3.2 Methods

3.3 Experimental design

The animals underwent AAV injection into the DRN on days 35 and 34 before stroke, which was followed by approximately one week of recovery (**Figure 3**). Then, the animals underwent daily training in the staircase test and weekly training in the irregular ladder rung. After 16 days of training, the animals were tested in the elevated plus maze (EPM) following a 1 mg/kg body weight dose of intraperitoneally injected CNO.

To determine the optimal dose for the experiment, the animals were also tested in the open field after administering CNO at doses of 0.1 mg/kg, 0.5 mg/kg, and 1.0 mg/kg body weight, with a one-day washout period between each testing session. Before the photothrombotic surgery was performed on day 0, a three-day washout period was implemented, during which food restriction was temporarily paused to ensure the animals were prepared for the surgery.

On day 1, 24 hours after photothrombotic surgery, a MRI scan was performed to evaluate the size and lesion of the photothrombotic stroke. CNO was administered intraperitoneally starting on day 1 and was continued daily until the completion of the experiment with perfusion on day 29. The food restriction was continued on day 2 after stroke. The critical period of rehabilitation in this type of study was defined as the first 4 weeks after stroke induction (day 1-28). Starting on day 3, all animals were tested three times a week in the staircase test. In the irregular ladder rung test, mice were assessed once a week.

The brains were harvested and sectioned for immunohistochemical analysis. In this experiment, three different groups were used: one group with DRN activation (hM3Dq), another with DRN inhibition (hM4Di), and a control group without DRN modulation

(EGFP). All groups were subjected to stroke, received CNO administration, and underwent identical training and testing procedures. The study was initiated with 13 animals in the hM3Dq group, 12 in the EGFP control group, and 10 in the hM4Di group. In this experiment, the hM3Dq group was intentionally overrepresented with 13 animals to enhance statistical power for detecting effects due to DRN activation, which is the primary focus of the study. Therefore, only 10 animals were allocated to the hM4Di group.

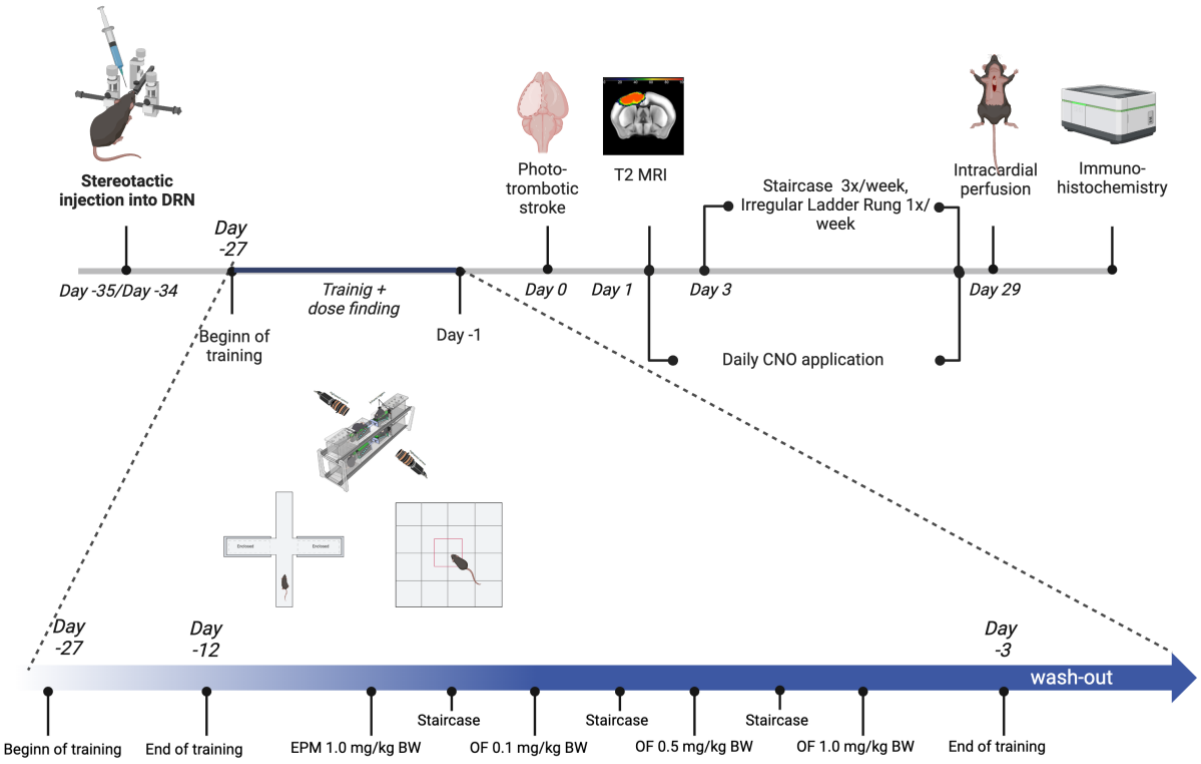

Figure 3. Experimental design. DRN: dorsal raphe nucleus, CNO: Clozapine N-oxide, OF = Open Field. Created with BioRender.com.

3.3.1 Sample size calculation

Given that there have been no comparable studies involving chemogenetic stimulation of neurons in the DRN in the context of stroke recovery, it was not possible to estimate the effect size in advance. The number of cases was determined to ensure sufficient precision in estimating the effects. The experiment followed a factorial design, focusing on the main effects of dosage and genotype. Based on prior experience with similar exploratory studies, we allocated 10 mice to each subgroup, resulting in a total of 30 mice (10 in the EGFP control group, 10 in the hM3Dq effector group and 10 in the hM4Di effector group). We anticipated a standard deviation of 0.3 times the mean (fold

regulation) in expression. Accounting for an estimated dropout rate of 15 % in stroke studies, the final total was adjusted to 35 animals. With this sample size, a two-sided 95 % confidence interval for the mean difference between three independent groups of 10 animals, assuming a pooled standard deviation of 0.3*mean, would extend plus/minus 0.27*mean around the observed mean difference (t-value of 2.4 with an alpha level of 0.03 and 18 degrees of freedom). A two-sided t-test with a significance level of 0.05 and a sample size of 10 animals per group was calculated to have approximately 90 % power to detect a standardized effect size (Cohen's d) of 1.7, according to G*power 3.1 software.

3.3.2 Method of blinding

The experimenters were blinded to group assignments and conducted all procedures at consistent time points daily, ensuring that each animal group underwent the same procedures at the same time of day. We performed data analysis without knowledge of the viral constructs used, ensuring objectivity in the results.

3.3.3 Method of randomization

Subjects were allocated to the different experimental groups using simple randomization. To control for sex-related bias, we included the same amount of male and female animals. Additionally, we minimized the number of individuals responsible for handling and conducting the behavioral experiments to reduce bias that could arise from variations in experimenter behavior or smell.

3.3.4 Exclusion criteria

Subjects that did not learn the staircase task will be categorized as non-learners. Only those demonstrating a pellet-reaching performance within 20 % of the standard deviation from the mean, approximately 60 % of the total achievable pellets per side, were included in the analysis. Animals with a stroke volume less than 6 mm^3 were excluded from the study. Additionally, animals that did not exhibit reporter expression in the DRN during histological analysis were excluded from the study.

Based on these criteria, within the hM3Dq group, two animals were excluded due to a lesion size < 5 mm^3, resulting in a group size of 11 animals. In the EGFP group, two animals were excluded due to the absence of a stroke, and two additional animals were excluded because of a lesion size < 5 mm^3, resulting in a group size of 8 animals. In the hM4D group, three animals were excluded due to complications during the AAV

injection, resulting in a total of seven animals. Details of these exclusions and the resulting group sizes are summarized in **Figure 4**.

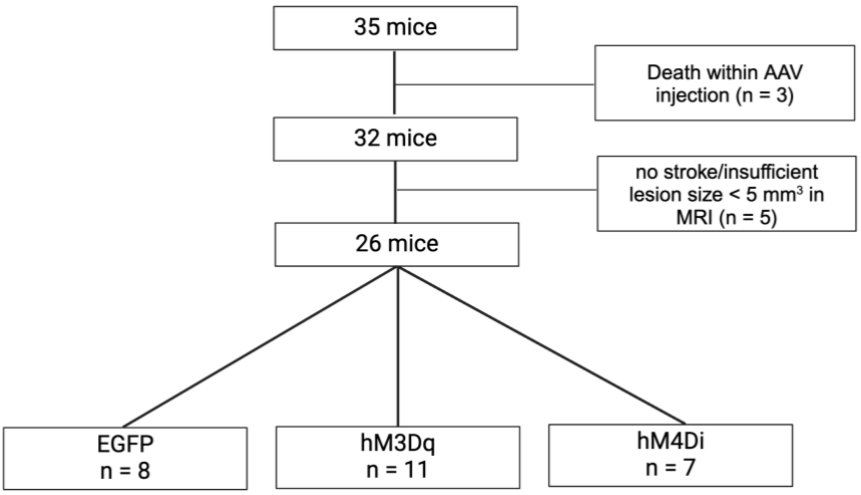

Figure 4. Animal exclusions and group sizes. Created with BioRender.com.

3.4 Animals

C57BL/6 mice from Charles River were used in this experiment. Subjects were between 12 and 14 weeks old when starting the experiments. The body weight was between 19 and 27 g. The animals were maintained on a non-reversed 12-hour light-cycle (light on from 06:00 - 18:00). Animals were housed with littermates (max. 5 subjects per cage). Cages were changed once a week. Animals were given housing and enrichment material. Animals were given ad libitum access to food (laboratory chow) and tap water during the recovery phase after surgery. During training and testing in the staircase task, mice were put under food restriction for 22 hours a day and were given laboratory chow for 2 hours per day after testing in the staircase. All animal procedures have been approved by the Berlin State Authority ("Landesamt für Gesundheit und Soziales", permit number: G 0173/20). The experiments adhered to the guidelines and recommendations set by the Federation of European Laboratory Animal Science Associations (FELASA) for the care and use of laboratory animals.

3.5 Implantation of an identification and temperature chip

We implanted a 14-mm radio frequency identification transponder chip under the skin on the back of the mice using isoflurane anesthesia (induction 2.5-3 %, maintenance 1-1.5 %; CP Pharma). This chip allowed for optimal and stress-free temperature monitoring and to verify the identity of the animals during daily documentation.

3.6 Stereotactic Adeno-Associated Virus (AAV) injection

Amido Daugardt, a medical doctorate candidate in the lab, and Dr. med. Leif Koschützke injected two different Adeno-associated viruses (AAVs) into the DRN using stereotactic surgery: rAAV-Tph2-Cre, serotype AAV2/9 in a 1:1 mixture with either pAAVhSyn-DIO-hM3D(Gq)-mCherry for the hM3Dq group, AAV9-hSyn-DIO-hM4d(Gi)-mCherry for the hM4Di group or pAAV-hSyn-DIO-EGFP for the control group.

For the procedure, mice were anesthetized using isoflurane (induction 2.5 - 3 %, maintenance 1 - 1.5 %; CP Pharma) and placed into a stereotactic frame. The scalp was shaved and covered with the local anesthetic bupivacaine for five minutes. An incision was made in the skin using a scalpel, and bregma and lambda points were identified and used as reference points. A precision drill was used to perforate the posterior skull based on coordinates relative to bregma in a minimally invasive way. To achieve injection into the DRN, the following coordinates were used: AP = -4.455 mm; ML = 1.100 mm; DV = 3.991 mm. Starting from bregma, the syringe was moved 4.455 mm posteriorly and 1.100 mm laterally to the right. At this precise point, the syringe was angled at 20° while maintaining its exact location. The syringe was positioned directly on the dura, and the exact DV value was noted. It was then moved 3.991 mm ventrally below the dura. A volume of 133 nl of the viral vector mixture (1:1 ratio of TPH2-Cre virus and Cre-dependent virus) was administered over five minutes. Following the injection, the syringe was retracted by 0.005 mm and left in place for an additional 5 minutes. The opened skin was then closed with double-knot sutures and the animals were administered subcutaneously with NaCl and 5 mg/kg body weight Carprofen. After being provided with wet food, the animals were placed in a warming cage set to a temperature of 28 - 30 °C for 1 hour. Once a stable condition was confirmed, the animals were returned to their respective home cages. During the intervention, body temperature was monitored and stabilized at 37.0 °C via TC-1000 system.

3.7 Photothrombotic surgery

The photothrombotic stroke model is an experimental method used to induce a localized stroke in animals. It is based on the principle that the photosensitive dye Rose Bengal, after being injected into the peritoneum of the animal, circulates throughout the bloodstream. When the targeted brain area is exposed to a specific light source, Rose Bengal promotes the production of reactive oxygen species, leading to damage

of the local endothelial cells, aggregation of platelets, and the obstruction of blood flow in the illuminated region (Labat-gest & Tomasi, 2013).

Amido Daugardt and I performed the photothrombotic surgery using a protocol based on the methods described by Bachmann et al. (2014). Mice were anesthetized using isoflurane (induction 2.5 - 3 %, maintenance 1 - 1.5 %). Before placing the mice in a stereotactic frame, 0.1 ml of 10 mg/ml Rose Bengal in 0.9 % NaCl solution was injected intraperitoneally. We exposed the skull through a midline incision in the scalp. Before placing an opaque squared aluminum frame that spares the motor cortex (i.e., rostral to caudal -2.5 to 2.5 mm, medial to lateral 0 to 3 mm in relation to bregma) (Tennant et al., 2011). The skull was wiped with cotton swabs to remove all connective tissue and wound fluid. This ensured that the placement of the template and the light path were not compromised. The frame had an opening of rostral to caudal 5 mm, and medial to lateral 3 mm. Seven minutes after intraperitoneal injection of 0.1 ml Rose Bengal (13 mg/kg body weight, 10 mg/ml Rose Bengal in 0.9 % NaCl solution), the light source was placed on the opening of the frame, ensuring no light gets past the aluminum frame and pushed carefully on the skull. We illuminated the skull with a cold light source that was attached to the stereotactic frame for 11 minutes. At the end of the light exposure, NaCl was dropped on the open part of the scalp to allow for cooling (10 -15 seconds) and was then wiped off to remove the frame. The scalp of the animal was sutured with double-knot sutures and 0.1 ml NaCl (0.9 %) and 0.1 ml Carprofen (5 mg/kg body weight) were given subcutaneously. Animals were allowed to recover on a heating pad for at least 2 hours. After being provided with wet food, the animals were placed in a warming cage set to a temperature of 28 - 30 °C for 1 hour. Once a stable condition was confirmed, the animals were returned to their respective home cages.

3.8 Magnetic Resonance Imaging

We performed MRI and acquired a T2-weighted image set 24 hours after the photothrombotic stroke surgery to allow for the assessment of stroke topology. For the procedure, mice were anesthetized with isoflurane in a 70:30-mixture of nitrous oxide and oxygen. The animals were placed in the holding chamber of a 7 Tesla MRI scanner. A T2-weighted 2D turbo spin-echo sequence was employed for imaging the mouse brain, with the following parameters: repetition time of 4200 ms, echo time of 36 ms, RARE factor of 8, 4 signal averages, 32 axial slices with a slice thickness of

0.5 mm, a matrix size of 256 x 256 and a field of view measuring 2.56 x 2.56 cm. Throughout the measurements, the breathing rate and body temperature of the mice were monitored, and the continuous flow rate of isoflurane was adjusted based on the breathing rate and pattern of the animal. The ANALYZE software was used to segment the hyperintense lesion. Hyperintense ischemic regions in the axial T2-weighted images were delineated using a region of interest tool. This tool facilitates threshold-based segmentation by linking all pixels within a defined threshold range around the selected seed pixel, resulting in a 3D object map of the stroke area. The software then automatically computed the total volume of this object map. Image processing and co-registration to the Allen Brain Atlas was performed using Fiji and custom-made analysis pipeline described recently (Knab et al., 2023; Koch et al., 2019; Skrobot et al., 2024).

3.9 Behavioral Tests

3.9.1 Open field

We performed the open field test, which is primarily used to assess general locomotor activity, exploration, and anxiety-like behavior (Tatem et al., 2014). The test took place in a large, open squared arena (500 x 500 mm) with high walls. Within the designated space, there were distinct inner and outer center areas clearly marked. The procedure was conducted following a published protocol by Tatem et al. (2014). We placed the animals of all groups in the middle of the inner center area and recorded for 10 minutes at 30 minutes after CNO administration. Three different doses of CNO – 0.1 mg/kg, 0.5 mg/kg, and 1.0 mg/kg body weight – were administered on separate days in the open field test to determine the optimal dosage. To assess and compare locomotor activity across the different dosages and groups, the total distance traveled was measured during this test using the AnyMaze software.

3.9.2 Elevated plus maze

We conducted the EPM test, which is designed to evaluate anxiety-like behavior in rodents (Walf & Frye, 2007). It consists of two open arms and two closed arms arranged in a plus-sign shape, elevated above the ground. The procedure was carried out according to a published protocol by Walf & Frye (2007). Animals were placed in the center of the maze, and their behavior was observed for five minutes at 30 minutes after CNO administration. In this experiment, the key parameters assessed were the

time spent in the open and closed arms, as well as the time spent in the center and compared across the different groups using the AnyMaze software.

3.9.3 Staircase task

We performed the staircase task, which is a sensitive method for detecting deficits in contralateral reaching performance following unilateral motor cortex lesions (Baird et al., 2001). The task setup included eight identical steps on each side of a central beam. Mice were placed into the chamber and recorded for 30 minutes. Performance in the staircase task was evaluated by conducting a conventional pellet count (20 mg sucrose), which accounts for the pellets remaining at the end of the task. We arranged four staircase boxes in a 2 x 2 grid on a customized platform (**Figure 5**). This platform allowed us to ensure the precise placement of each staircase box across different testing days. Each apparatus consisted of two chambers: a resting chamber and a reaching chamber, which contained two staircases with eight steps each, separated by a central beam. Each stair step was 8 mm wide and contained a well with a diameter of 6 mm and a depth of 3 mm, filled with a pellet.

The procedure followed a protocol recently published (Knab et al., 2023). The experimental animals underwent food restriction to increase their motivation to grab pellets from the wells in the steps. The food restriction began three days before the start of staircase training. The animals were trained daily for 16 days in the staircase apparatus, where they learned to grasp and eat pellets with their left and right forepaws separately for 30 minutes. For assessing the performance of the mice in the staircase task, we counted the remaining pellets in each staircase box at the end of each trial. This was used to check whether mice were reaching a stable plateau. After completing the training, the food restriction was paused to allow the mice to reduce stress before stroke. After recovering from the stroke surgery, food restriction was resumed, and the mice underwent staircase testing three times a week. On each test day, the pellets successfully grasped were counted after a period of 30 minutes.

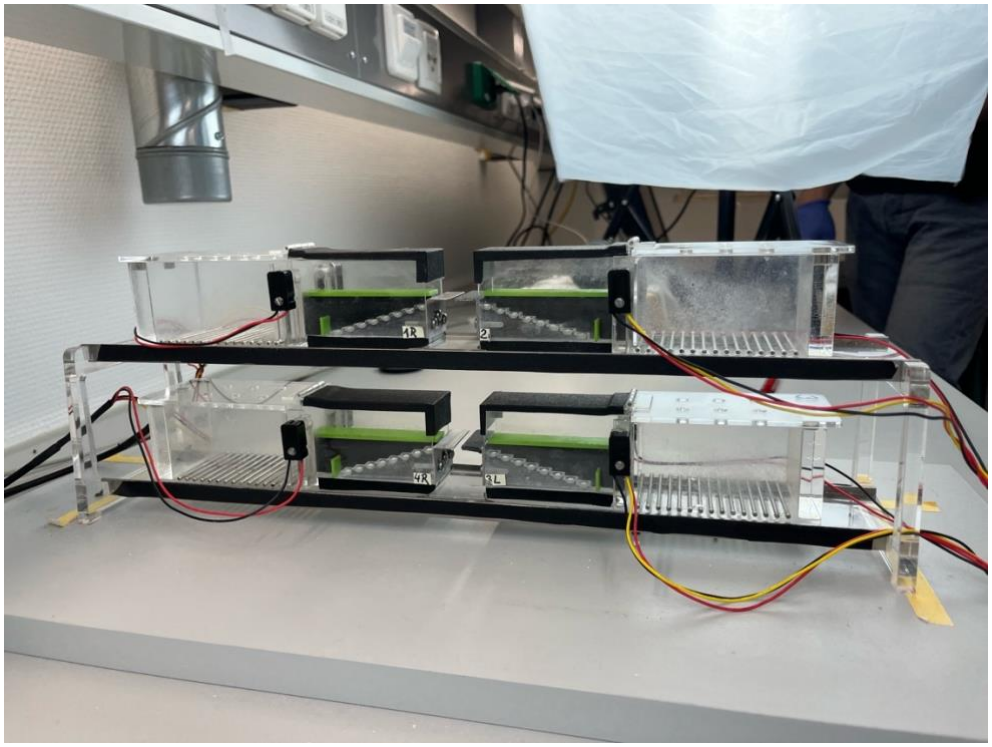

Figure 5. Experimental staircase setup in the group of AG Harms.

3.9.4 Irregular Ladder Rung test

The irregular ladder rung task is designed to evaluate skilled walking in mice (Metz & Whishaw, 2009). In this task, the mice traverse a horizontal ladder with a length of approximately 70 cm three times with irregular rung spacing (1-2 cm spacing, 1 mm diameter of the rungs; **Figure 6**). This variation in rung spacing prevents the mice from memorizing the specific positions of the rungs, thereby reducing their ability to compensate for impairments through learning (Metz & Whishaw, 2009).

The procedures were adapted according to a protocol that is already published (Weber et al., 2022). During the test, mice were filmed with a camera from underneath the apparatus and two angled mirrors on the side of the apparatus allow for additional filming of the posture of the animals from the right and the left side of the body. Mice were trained once a week on the irregular ladder rung for 3 weeks prior to stroke induction and recorded for baseline level of performance on the last training day before stroke. Following the stroke, their performance was evaluated once a week. The analysis of the irregular ladder rung test focused on baseline, day 4 and day 23, for evaluating the immediate post-stroke deficit and recovery towards the end of the experiment.

The videos from the Irregular Ladder Rung test were analyzed using DeepLabCut (DLC, v. 2.1.5), an algorithm designed for markerless and automatic tracking of pre-

defined body parts (Mathis et al., 2018). Being pre-trained on ImageNet, a widely used image recognition database, DeepLabCut only requires a small number of training video frames to automatically track specific body parts. In these training video frames, Hannes Diestelmeier, an intern in the lab, manually labeled 10 body parts (head, front toe tip, wrist, shoulder, elbow, back toe, back ankle, iliac crest, hip, and tail) in the side view perspective and eight body parts (head, right front toe, left front toe, center front, right back toe, left back toe, center back, tail base) in the bottom view perspective (**Figure 6**). These labeled video frames were used to train a neural network. To enhance accuracy, three rounds of refinement were conducted, during which any incorrectly or inaccurately placed markers tracking specific body parts were corrected. These corrections were subsequently used to retrain the neural network, leading to more precise automatic labeling.

Once the network was adequately trained, it automatically tracked features in new video recordings. The network predicted the marker positions in the new videos and created a CSV file with video pixel coordinates of the labels that were further processed for performance evaluation with custom scripts in R Studio (Version 4.04; Weber et al., 2022). This allowed us to identify stepping errors in the side view by effectively tracking the forelimbs and hindlimbs. A stepping error was defined when the toe tips of the mouse descended 0.5 cm or more below the height of the ladder. The code's accuracy was evaluated by comparing it to the gold standard of manual counting performed by human annotators. Yvonne Khor, a bachelor student in the lab, manually counted the stepping errors of the left and right front paws on baseline, day 4 and 23 of the testing period.

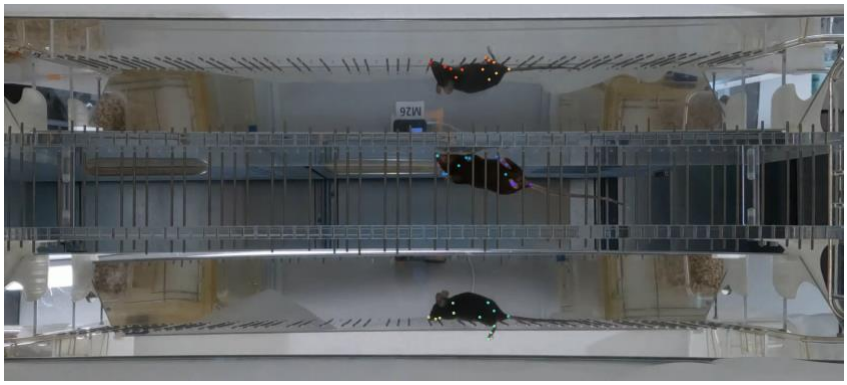

Figure 6. Irregular ladder set up in AG Harms with manually labeled body parts.

3.10 Transcardial perfusion

For transcardial perfusion, we anesthetized the mice via intraperitoneal injection of a ketamine (180 mg/kg body weight) and xylazine (20 mg/kg body weight) mixture. We monitored the depth of anesthesia by ensuring the absence of the toe-pinch reflex. We prepared the mice for intracardial perfusion by exposing the heart, inserting a cannula, and opening the right atrium to allow for efficient blood and perfusate clearance. We performed perfusion using a peristaltic pump, starting with 1x PBS for two minutes, followed by 4 % PFA. PFA was administered at a gradually decreasing flow rate: 9 ml/min for the first minute, 7.7 ml/min for the second minute, 7 ml/min for the third minute, 6 min for the fourth minute, and finally 5.7 ml/min for four minutes. We extracted the brains placed them in 4 % PFA for 24 hours. Subsequently, the tissues were stored in 1x PBS at 4 °C.

3.11 Histological analysis

We dissected the brains in 50 µm-thick sections using a Leica VT 1000s vibratome. The brain slices were then stored 48-well plates in 1x PBS containing 1 % sodium azide at 4 °C. We collected sections from each animal at the level where the DRN has its biggest configuration (spanning 4.10 to 4.80 mm posterior to the bregma (Huang et al., 2019)). We washed the slices three times for five minutes each in 1x PBS, followed by a 1-hour blocking step in a solution of 10 % NDS) and 1 % Triton X-100 in 1x PBS. The primary antibodies anti-cFOS rabbit polyclonal and anti 5-HT goat polyclonal were diluted 1:1000 in a solution containing 500 µl of 1 % NDS and 0.1 % Triton X-100 in 1x PBS solution. The slices were incubated overnight in this primary antibody solution at 4 °C. After incubation, we washed the slices three times for 5 minutes in 1x PBS. We diluted secondary antibodies donkey anti-rabbit Alexa 488 and donkey anti-goat Alexa Fluor Plus 647 for the hM3Dq and hM4Di group and donkey anti-rabbit Alexa Fluor 546 and donkey anti-goat Alexa Fluor Plus 647 for the EGFP group 1:400 in 1 % NDS and 0.1 % Triton X-100 in 1x PBS solution. We incubated the slices in this secondary antibody solution for 2 hours. Then, we washed the slices three times for five minutes in 1x PBS and incubated them for 1 hour in DAPI (1 µg/ml in 1x PBS).

We acquired immunofluorescence images using a spinning disk confocal microscope (Opera Phenix High-Content Screening System) with 2 µm-thick planes, using 20x magnification (N.A.: 0.75, water immersion). We employed laser diode wavelengths of 461, 488, 561, and 647 nm for DAPI, cFOS, mCherry (DREADDs), and 5-HT,

respectively in the hM3Dq and hM4Di group. In the EGFP group, the same wavelengths were used for DAPI, EGFP, cFOS and 5-HT. This setup produced an average z-optical section of 20 µm. All images were composed of multiple fields, and for each of them, an image that represented the maximum intensity value of each pixel from a stack of images was acquired through a custom-made python script. These fields were stitched together in ImageJ/FIJI. Contrast and brightness settings were adjusted to highlight stained areas. This was done for every channel separately. All channels were then merged in a composite file to verify the expression and location of the DREADDs. The images showing cFOS expression were subsequently analyzed in ImageJ/FIJI to quantify the number of cFOS-positive cells, enabling the comparison of activity levels across different groups. First, the images were converted to grayscale, and the auto local thresholding using the Bernsen method with a radius of n = 15 was applied. The images were then binarized and converted into masks. To separate clumped cells, the watershed algorithm was used. Particle analysis was performed with a pixel size range of 10-2000 µm² and a circularity of 0.00 - 1.00.

3.12 Statistical analysis

We performed statistical analysis using GraphPad Prism v10. All data was expressed as mean ± 95 % confidence interval (CI). The data was tested for Gaussian distribution using the Shapiro-Wilk test and for variance homogeneity using the Brown-Forsythe test. The data for the distance traveled in the open field was logarithmically transformed to achieve a normal distribution. To analyze differences between treatment groups, we used a two-way repeated measures analysis of variance (ANOVA) for the distance travelled in the open field and the reached pellets during staircase testing after stroke. Tukey's post-hoc test was applied to further evaluate differences in distance traveled and Dunnett’s post-hoc test for post-stroke staircase performance. One-way ANOVA was conducted to assess differences in stroke volume and stepping errors on day 23 between the EGFP, hM3Dq, and hM4Di groups, while post stroke stepping errors within each group were compared using a one-way repeated measures ANOVA with Tukey's post-hoc test. For the EPM and cFOS cell counting, we conducted Kruskal-Wallis tests followed by Dunn’s post-hoc test. A linear regression analysis was performed to compare the manual and automated counts of stepping errors in the irregular ladder rung task. The level of significance was set at < 0.05.

4 Results

4.1 Development of a mouse model to induce serotonergic transmission from the dorsal raphe nuclei

First, we developed a mouse model that allows us to induce serotonergic transmission from the DRN. Therefore, AAVs coding for DREADDs or EGFP were stereotactically injected in the DRN. The hM3Dq-DREADD was used to stimulate neuronal activity. EGFP was used as negative control, while the hM4Di DREADD was used to inhibit neuronal activity. The DREADDs were fluorescently tagged with mCherry. A TPH2 promoter was used to ensure specific expression of the DREADDs in serotonergic neurons.

We validated the DREADDs or EGFP expression in the DRN by performing histological analysis on midbrain slices where the DRN has its largest configuration (spanning 4.8 to 4.1 mm posterior to the bregma) (**Figure 1**). Successful transduction was detected using the mCherry (DREADDS) or EGFP (negative control) signals, respectively, both shown in magenta false color. We were able to validate that the DREADDs as well as EGFP were expressed in the DRN. However, we also observed that the expression patterns varied among experimental subjects, and there may be variance in the exact location within the DRN. Additionally, we stained for serotonin (5-HT, white signal) to identify serotonergic neurons. A partial overlay between serotonin and DREADDs expression was found. Therefore, we were able to transduce serotonergic neurons in the DRN with the DREADDs.

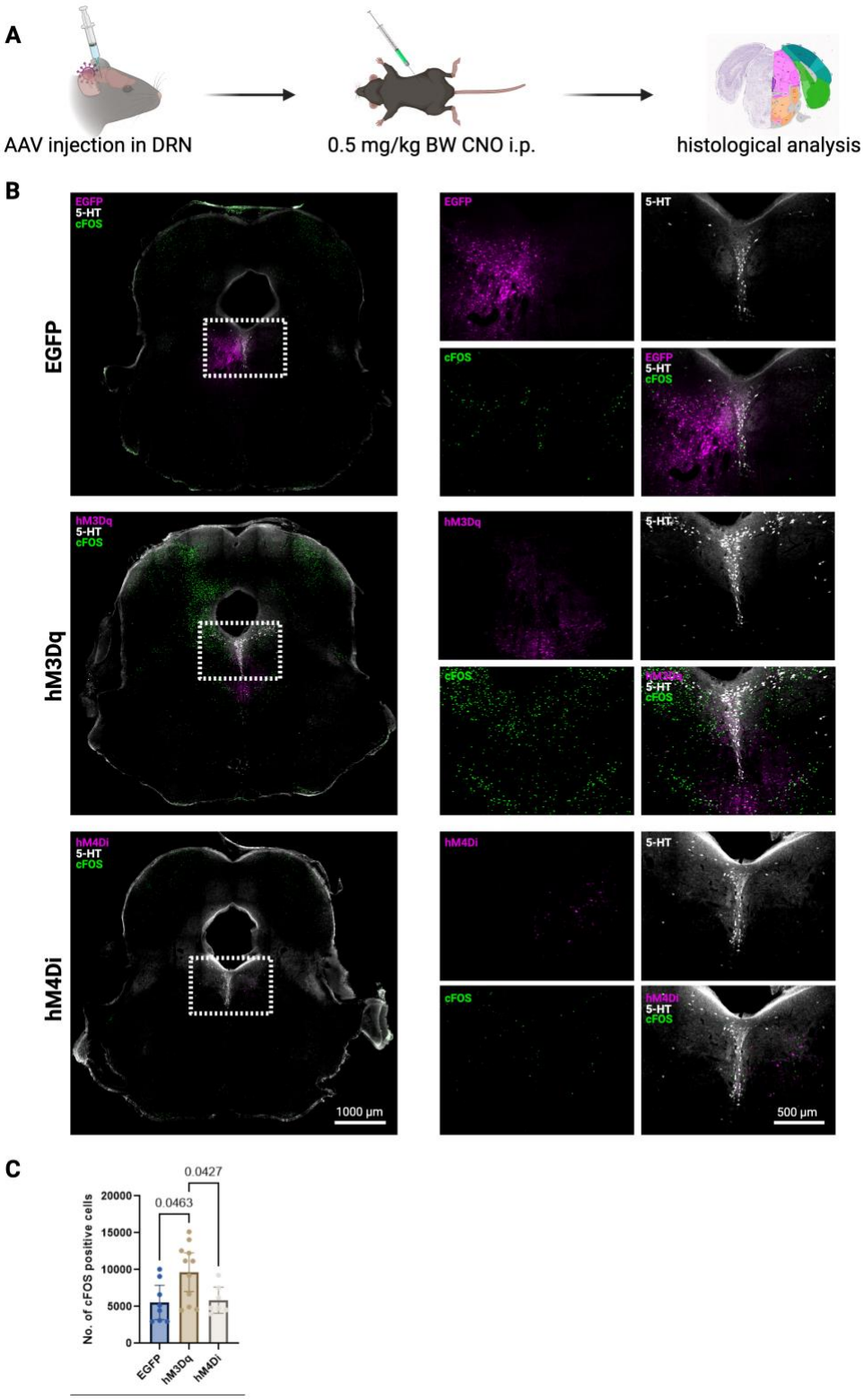

Figure 7. Immunohistochemistry of midbrain slices validating DREADD expression in the DRN. **A.** Scheme of experimental procedure: CNO administration 30 minutes prior to sacrificing the animals with subsequent histological analysis. **B**. Representative images of the EGFP, hM3Dq, and hM4Di group. The dashed white rectangle indicates the location of the DRN, with a close-up view presented on the right side. **C.** Increase of cFOS-positive cells in the hM3Dq group compared to the EGFP, and hM4Di group. Welch's ANOVA test W(2, 15.11) = 4.259, *P* = 0.0341 with Dunnett's post-hoc test.

4.2 Quantitative differences in cFOS expression

Next, we investigated whether DREADD activation with CNO leads to either induced (hM3Dq), reduced (hM4Di) or unchanged (EGFP) neuronal activity. The green signal in **Figure 1** marks the presence of cFOS, a protein commonly used as a marker for neuronal activity (Hudson, 2018). Cells stained green indicate that they were engaged in neural activity at the time of death. Before being sacrificed, the animals received an application of CNO (0.5 mg/kg body weight). For cell counting analysis, one standardized slice (as stated above) for each animal participating in the study was used. We counted and compared cFOS-positive cells across all groups using the ImageJ/FIJI function “analyze particles” (**Figure 1**). Welch’s ANOVA test revealed a statistically significant difference between the groups ($p = 0.0341$). Subsequent Dunnett’s post-hoc analysis indicated that the hM3Dq group had a significantly higher mean rank of c-FOS-positive cells compared to the EGFP group (mean rank difference = 4108, $P = 0.0463$ and hM4Di group (mean rank difference = 3802, $P > 0.0427$). No significant differences were observed between the EGFP and hM4Di group (mean rank difference = -306.1, $P = 0.9919$). These findings demonstrate that the hM3Dq treatment successfully led to a stronger cellular response compared to the EGFP group, achieving the intended enhanced activation.

4.3 DRN serotonergic transmission on behavior increased anxiety related behavior and decreased locomotion

Then, we tested the effectiveness of our mouse model to change behavior associated with DRN serotonergic transmission. Literature indicates that increased DRN serotonergic transmission reduces locomotor activity (Kalueff et al., 2007; Ren et al., 2018) and elevates anxiety-related behaviors (Ren et al., 2018), while DRN lesions tend to reduce anxiety-like behaviors (Sena et al., 2003). We used the distance travelled in the open field as an outcome measure for locomotor activity and the EPM test to assess the anxiety-like behavior. We administered 1.0 mg/kg body weight of CNO to all experimental animals, as this dosage is commonly used in the literature (Manvich et al., 2018). The open field test and EPM were performed 30 minutes after administration. **Figure 8** shows the time spent by each group in the center, closed arms and open arms, respectively.

We conducted a Kruskal-Wallis test to determine whether the time spent in each location of the EPM and distance travelled in the open field differs among the different genotypes in response to the 1 mg/kg body weight treatment with CNO. No significant difference was found in the time spent in center ($P = 0.6469$) and in the closed arms ($P = 0.1411$) among the groups. However, a significant difference in the time spent in open arms was observed among the different genotypes ($P = 0.0007$). Post-hoc Dunn's test showed that the hM3Dq group spent significantly less time in the open arms compared to EGFP (mean rank difference = -11.62, Z = 3.270, $P = 0.0032$) and hM4Di (mean rank difference = -11.54, Z = 3.121, $P = 0.0054$). No significant differences were found between hM4Di and EGFP (mean rank difference = -0.0804, Z = 0.0203, $P > 0.9999$).

A significant difference in the distance traveled in the open field test was observed among the genotypes ($P = 0.0245$). Dunn's post-hoc analysis revealed that the hM4Di group traveled significantly more compared to the hM3Dq group (mean rank difference = 9.714, Z = 2.627, $P = 0.0259$). However, no significant differences were found between hM3Dq and EGFP (mean rank difference = -6.125, $P = 0.2544$), or between hM4Di and EGFP (mean rank difference = 3.589, $P > 0.9999$).
By demonstrating that the hM3Dq group showed reduced locomotor activity and spent significantly less time in the open arms of the EPM compared to the EGFP and hM4Di group, indicating heightened anxiety-like behavior, we were able to validate that induction of our mouse model leads to DRN serotonergic transmission-like behavioral effects.

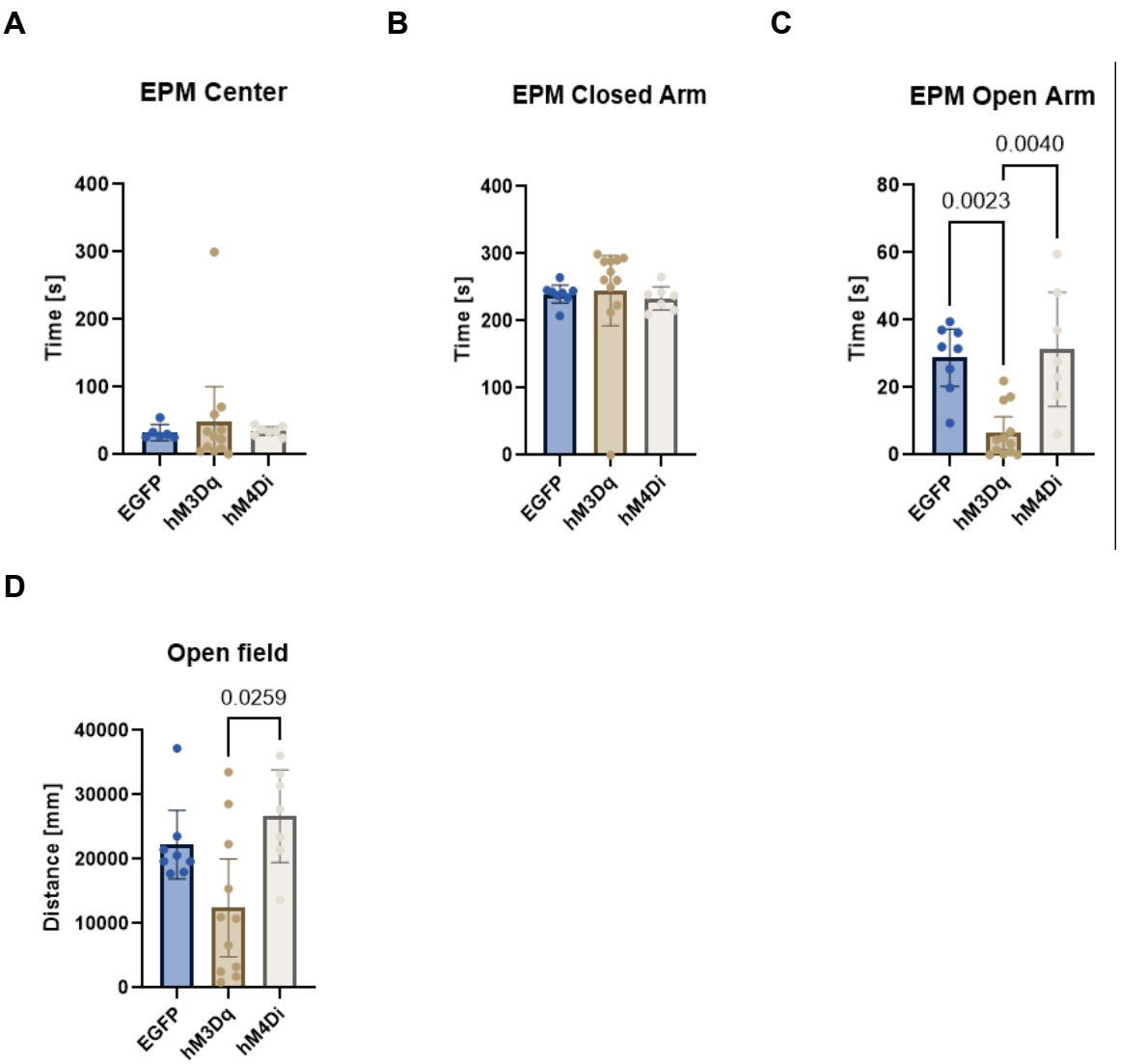

Figure 8. DRN serotonergic transmission increased anxiety-related behavior and decreased locomotion following administration of 1 mg/kg body weight CNO in the EPM and open field. **A.** No significant differences between EGFP, hM3Dq, and hM4Di groups in the time spent in center. Kruskal-Wallis test $\chi^2(2, N = 25) = 1.35$, $P = 0.5084$. **B.** No significant differences between EGFP, hM3Dq, and hM4Di groups in the time spent in closed arms. Kruskal-Wallis test $\chi^2(2, N = 27) = 4.91$, $P = 0.0857$. **C.** hM3Dq group spent significantly more time in the open arms compared to the EGFP- and hM4Di group. Kruskal-Wallis test $\chi^2(2, N = 27) = 15.63$, $P = 0.0004$ followed by Dunn's post-hoc test. **D.** hM3Dq group showed significantly less distance travelled in the open field compared to the hM4Di group. Kruskal-Wallis test: $\chi^2(2, N = 26) = 7.42$, $P = 0.0245$ followed by Dunn's post-hoc test.

4.4 Dose finding

After validating DRN serotonergic transmission, we next aimed to determine an optimal dose of CNO that would provide the maximum effect in DRN activity modulation while producing minimal side effects. Given that reduced locomotor activity and anxiety-like behavior can impair performance in behavioral tests, we investigated whether administering CNO in the afternoons 12 hours before testing had potential side effects on motor tests that could last until the next day. We performed the open field test 30 minutes after CNO administration to monitor whether the CNO dose still influences

DRN activation. The staircase test was performed the next morning. The CNO doses administered were 0.1 mg/kg, 0.5 mg/kg, and 1.0 mg/kg body weight (**Figure 11**). All three groups received each of the three dosages on separate days, with one day washout period between each dosing session.

The requirement for detecting side effects in the staircase task was the successful learning of this behavioral test by all mice among the different groups. To evaluate the learning and task acquisition of mice, the reached pellets, presented as a percentage of their individual baseline performance, were monitored starting from the first day of staircase training (day -27 before stroke). The baseline was determined by averaging the performance over a seven-day period before the stroke (days -18 to -12), during which mice achieved stable performance levels (**Figure 9**). CNO was not yet administered as these were the training sessions. We have visualized the data for illustration purposes only, without conducting any statistical tests. No noticeable differences were observed in how the different groups learned the task over time. We observed the establishment of a performance plateau in the staircase test, confirming that the mice had successfully learned the task, with no differences in learning observed across the different groups.

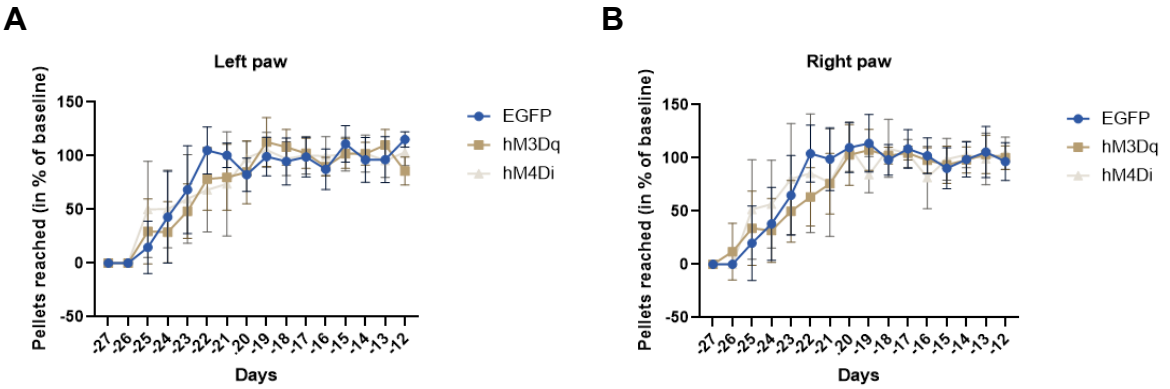

Figure 9. Performance improvement in the staircase test over time with a plateau reached by day -18 for the left and the right paw in the EGFP, hM3Dq, and hM4Di groups. A. Pellets reached (in % of baseline) with the left paw during the first 16 days (day -27 to day -12) of staircase training in EGFP, hM3Dq, and hM4Di group. **B.** Pellets reached (% of baseline) with the right paw during the first 16 days (day -27 to day -12) of staircase training in EGFP, hM3Dq, and hM4Di group.

To assess the effects of DRN activation on the distance travelled in the open field, we conducted a two-way repeated measures ANOVA to examine the effects of dosage and genotype, after logarithmically transforming the data to achieve normal distribution (**Figure 10A**). The analysis revealed no significant interaction between dosage and genotype (4.84 %, of total variation, $F(4, 46) = 1.78$, $P = 0.1486$), indicating that there is no evidence for a dose-response relationship in the distance traveled that depends

on the genotype. Additionally, there were no significant effects of dosage (2.40 % of total variation, F(1.52, 35.0) = 1.77, *P* = 0.1912). However, there was a significant effect of the genotype (22.5 % of total variation, F(2, 23) = 6.91, *P* = 0.0045), indicating that genotype significantly influences the distance traveled. We depicted the non-logarithmic data to illustrate the raw values for easier visualization (**Figure 10B**).

To further determine specifically where the differences lie among the groups or dosages, we performed a Tukey post-hoc analysis. The distance traveled was reduced in the hM3Dq group compared to the EGFP group by 12 708 mm and in the hM4Di group by 15 353 mm after receiving 0.5 mg/kg body weight CNO, suggesting that the activation of the hM3Dq receptor following CNO administration accounts for reduced locomotor activity in the open field test. No significant differences were observed between the hM4Di and EGFP group at any dosage of CNO, while also no significant effects were seen within the hM4Di group across the different dosages, indicating that the activation of the hM4Di receptor with CNO does not alter the locomotor activity of mice in the open field test at the dosages tested. Within the EGFP group, a slight reduction by 3 114 mm in distance traveled was noted at a dosage of 1.0 mg/kg body weight compared to 0.5 mg/kg body weight, which was however not significant in the logarithmic data. Within the hM3Dq group, a reduction in the distance traveled compared to 0.1 mg/kg body weight was observed at 0.5 mg/kg body weight (mean difference = -10 605 mm) and 1.0 mg/kg body weight (mean difference = -10 843 mm), which was, however, not significant in the logarithmic data. In addition, there was no statistically significant additional reduction in distance traveled between 0.5 and 1.0 mg/kg body weight (mean difference = 238 mm), indicating that the 0.5 mg/kg body weight dosage may already achieve a ceiling effect on locomotor activity. Thus 0.5 mg/kg body weight may be sufficient to fully stimulate DRN serotonergic transmission.

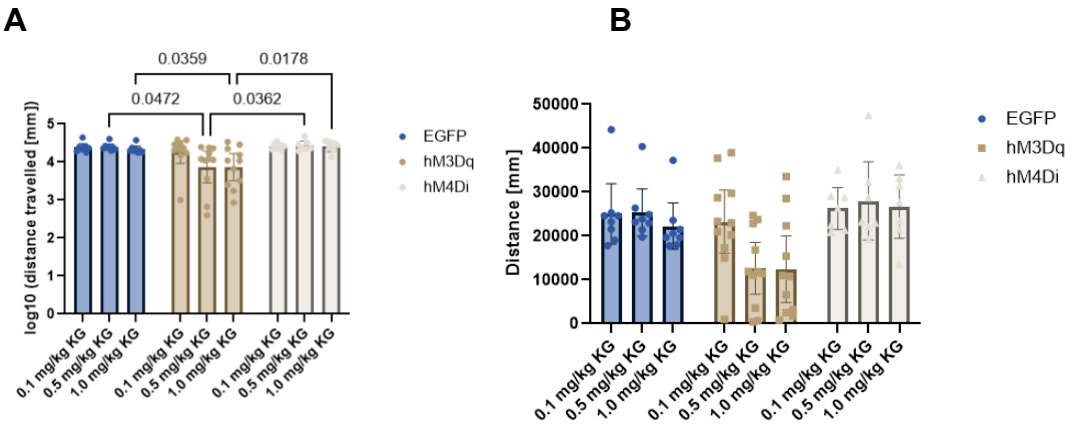

Figure 10. The distance travelled was reduced in the hM3Dq group at CNO dosages of 0.5 and 1.0 mg/kg body weight. **A.** The figure shows the logarithmic distance traveled in the open field test at CNO dosages of 0.1, 0.5, and 1.0 mg/kg body weight across EGFP, hM3Dq, and hM4Di groups. Two-way repeated measures ANOVA (dosage x genotype: 4.84 %, of total variation, $F(4, 46) = 1.78$, $P = 0.1486$; dosage: 2.40 % of total variation, $F(1.52, 35.0) = 1.77$, $P = 0.1912$; genotype: 22.5 % of total variation, $F(2, 23) = 6.91$, $P = 0.0045$) with Tukey post-hoc test. **B.** The figure shows the distance traveled in the open field test at CNO dosages of 0.1, 0.5, and 1.0 mg/kg body weight across EGFP, hM3Dq, and hM4Di groups.

Next, we determined whether any of the administered CNO dosages affects the staircase performance the following morning, approximately 12 hours after administration of 0.1, 0.5, and 1.0 mg/kg body weight CNO (**Figure 11**). Performance was measured as the number of pellets successfully retrieved with both left and right paws within 30 minutes and presented as a percentage of their baseline performance (the average number of pellets retrieved during seven days (day -18 – day -12) of the plateau phase). All mice received all three different dosages of CNO at separate time points (as shown in **Figure 10**).

To test for differences in staircase performance one day after the different dosages of CNO compared to baseline assessment, we performed Two-way repeated measures ANOVA. The primary source of variation was attributed to individual subject differences, accounting for 45.5 % ($F(23, 69) = 1.70$, $P = 0.0001$) of the total variation. In contrast, neither the interaction between dosage and genotype (3.80 % of total variation, $F(6, 69) = 1.00$, $P = 0.4319$) nor the effects of dosage (0.0284 % of total variation, $F(2.39, 54.9) = 0.0149$, $P = 0.9926$) or genotype (6.73 % of total variation, $F(2, 23) = 1.70$, $P = 0.2052$) alone were statistically significant. These results suggest that none of the dosages of CNO had a significant impact on staircase performance in any of the groups the following day.

The dose-response relationship observed in the hM3Dq group, where both 0.5 and 1.0 mg/kg body weight dosages led to significant reductions in activity compared to 0.1 mg/kg body weight (as shown in **Figure 10**), suggests that 0.5 mg/kg body weight

may be sufficient to achieve near-maximal receptor activation, with no further significant reduction at the higher dosage. This plateau indicates a potential ceiling effect in receptor-mediated suppression of locomotor activity, while not showing any negative effects on staircase performance the following day, establishing 0.5 mg/kg body weight as an effective dose in our experiment. Moreover, the reduction in locomotor activity seen in the EGFP group at the 1.0 mg/kg body weight dosage suggests that side effects may occur at this higher dose.

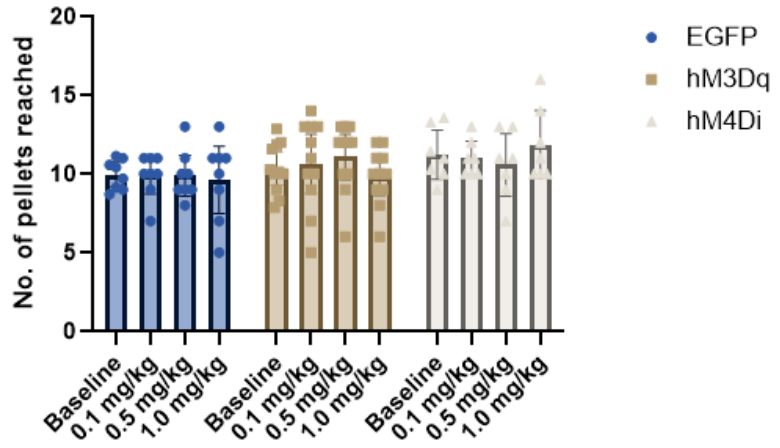

Figure 11. No significant effect of CNO dosages (0.1, 0.5, and 1.0 mg/kg body weight) on staircase test performance the following morning in EGFP, hM3Dq, and hM4Di group. Two-way repeated measures ANOVA (dosage x genotype: 3.80 % of total variation, F(6, 69) = 1.00, *P* = 0.4319; dosage: 0.0284 % of total variation, F(2.39, 54.9) = 0.0149, *P* = 0.9926; genotype: 6.73 % of total variation, F(2, 23) = 1.70, *P* = 0.2052).

4.5 Lesion size and location

Our aim was to determine the effect of DRN serotonergic transmission on stroke recovery. Therefore, we used the model of photothrombosis to induce a stroke. We induced a lesion in the left motor cortex of the mice, consequently expecting the contralateral right paw to be paretic. We acquired T2-weighted images using a 7 Tesla MR scanner to assess the location of the stroke and ensure consistent lesion volume across all animals. Achieving homogenous stroke volumes across all animals is crucial for the reliability and reproducibility of the experimental outcomes. Animals with lesion volumes less than 5 mm^3 as well as those in which stroke induction was unsuccessful were excluded from the experiment.

Based on these criteria, two animals had to be excluded due to small stroke volumes and two did have a stroke induction at all. Otherwise, the photothrombotic stroke model utilized in this study successfully induced homogeneous lesion sizes with a mean of

19.42 mm³ (σ = 4.319, $\sigma_{\bar{x}}$ = 0.8470) in all experimental animals, specifically targeting the left M1 motor cortex (**Figure 12**). To determine whether there were any differences in stroke volume between the groups, we performed a one-way ANOVA. No significant differences in stroke volume were detected across the groups (*P* = 0.881s), assuring homogeneity in lesion size.

A

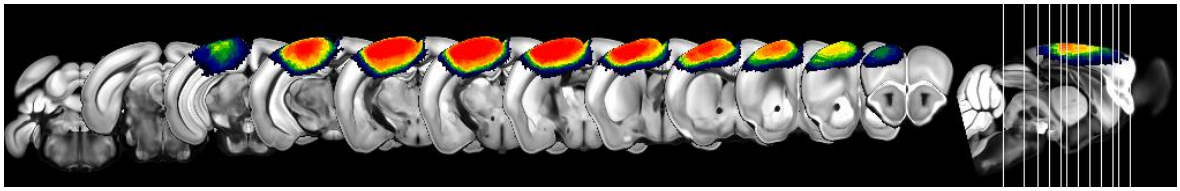

B

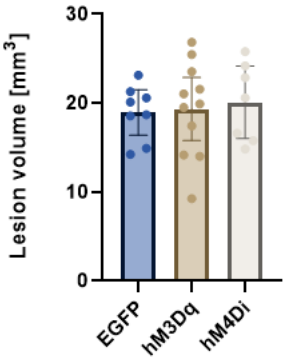

Figure 12. Homogenous stroke lesion volume and location across all animals. A. T2-weighted imaging showing lesion size and location acquired using a 7 Tesla MR scanner. Descriptive statistics: average lesion volume = 19.42 mm^3, σ = 4.319, $\sigma_{\bar{x}}$ = 0.8470, n = 26. **B.** No significant differences in stroke volume across EGFP, hM3Dq- and hM4Di groups. One-way ANOVA: F(2, 23) = 0.1279, *P* = 0.881.

4.6 DRN serotonergic transmission improves recovery after stroke

We examined the effect of post-stroke DRN serotonergic transmission on functional recovery using the staircase task and irregular ladder rung test. We induced DRN serotonergic transmission beginning one day after stroke by daily administration of 0.5 mg/kg body weight CNO in the afternoon. In the following mornings, the staircase test was performed three times a week after stroke over a period of four weeks (day 3 – day 28) and once a week in the irregular ladder rung test.

In the staircase task, performance measured by the number of pellets retrieved was assessed and expressed as the percentage of the baseline (performance in the period of day -18 – day -12) (**Figure 13**). We analyzed the data of the staircase test on the respective testing days across the four-week period using a two-way repeated

measures ANOVA for the ipsilateral left paw and the contralateral right paw followed by Dunnett's post-hoc analysis. We observed a significant effect of time, accounting for 12.9 % of the total variation in the ipsilateral paw ($F(7.20, 166) = 4.22$, $P = 0.0002$) and 21.3 % in the contralateral paw ($F(6.05, 139) = 8.01$, $P < 0.0001$), with the larger variation in the contralateral paw attributed to a greater initial decrease in performance following the stroke. However, there was no significant effect of genotype neither for the ipsilateral paw (0.0701 % of total variation, $F(2, 23) = 0.0956$, $P = 0.9092$) nor for the contralateral paw (0.0091 % of total variation, $F(2, 23) = 0.0077$, $P = 0.9923$). Moreover, there was no significant interaction between time and genotype for the ipsilateral paw (7.23 % of total variation, $F(36, 414) = 1.18$, $P = 0.2198$) and the contralateral paw (3.14 % of total variation, $F(36, 414) = 0.590$, $P = 0.9727$). These results indicate that the different groups did not recover differently. We observed a larger initial decrease in performance in the contralateral paw, which reflects the initial motor deficit caused by the stroke.

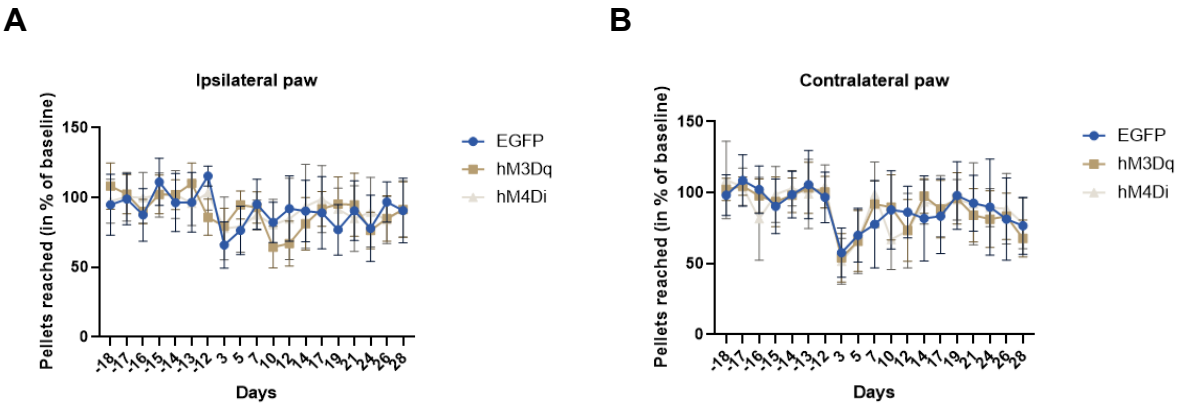

Figure 13. Decrease in staircase performance on day 3 following stroke for the left paw in the EGFP group and for the right paw in the EGFP, hM3Dq, and hM4Di group. A. Staircase performance of the ipsilateral left paw. Two-way repeated measures ANOVA with Dunnett's post-hoc test (time x genotype: 7.23 % of total variation, $F(36, 414) = 1.18$, $P = 0.2198$; time: 12.6 % of total variation, $F(7.20, 166) = 4.22$, $P = 0.0002$; genotype: 0.0701 % of total variation, $F(2, 23) = 0.0956$, $P = 0.9092$). **B.** Staircase performance of the contralateral right paw. Two-way repeated measures ANOVA with Dunnett's post-hoc test (time x genotype: 3.14 % of total variation, $F(36, 414) = 0.590$, $P = 0.9727$; time: 21.3 % of total variation, $F(6.05, 139) = 8.01$, $P < 0.0001$; genotype: 0.0091 % of total variation, $F(2, 23) = 0.0077$, $P = 0.9923$).

For the irregular ladder rung, baseline data were collected on day -13. We assessed recovery within each group by examining the total number of stepping errors at days 4 (initial deficit) and day 23 (recovery), as they represent the most critical time points, and compared them to the baseline. Analyzing these specific days allowed us to better detect subtle differences in motor recovery between groups while reducing potential

variability or noise from intermediate testing days that may not provide as clear insights into the recovery process.

To first validate the accuracy of the automatically counted stepping errors in our setup, stepping errors were manually counted at baseline, days 4 and 23. A regression analysis was then conducted to evaluate the accuracy of the automatically detected stepping errors. When comparing the automated count to the manual count for the contralateral paw, the regression analysis revealed a statistically significant relationship between manual and automated stepping error counts ($Y = 0.4354X + 0.5637$, $P < 0.0001$) (**Figure 14A**). The relationship was relatively strong, with the automated counts explaining a significant portion of the variance in the manual counts ($R^2 = 0.2575$), indicating that the automated detection system accurately captured the variability observed in the manual counts. However, the script failed to accurately detect stepping errors for the left paw, resulting in almost no errors being recorded. Regression analysis resulted in the following equation: $Y = 0.02342X - 0.0024$. A p-value of 0.1700 indicates that there was no meaningful linear relationship between the manual and automated counts for the left paw (**Figure 14B**). The R^2 value of 0.0246 shows that only 2.46 % of the variance in the manual counts is explained by the automated counts, further emphasizing the weak correlation. This discrepancy is likely due to a hardware issue caused by the suboptimal positioning of the mirror reflecting the left side of the mice, which affected the detection of the left paw during the test.

As a result, stepping errors on the left side were not reliably recorded. The setup was primarily focused on capturing movements on the right side, where we expected more changes, and the left side data was therefore not considered valid for analysis. However, for the paretic right side, the script was highly valid. Therefore, our analysis focused exclusively on the irregular ladder rung test results for the paretic right forepaw.

Figure 14C-E show the stepping errors in the irregular ladder rung task of the EGFP, hM3Dq and hM4Di group at baseline, days 4 and 23 of the contralateral paw. To assess recovery in each group separately we performed one-way repeated measures ANOVA with Tukey's post-hoc test. No significant differences were observed across time points in the EGFP group ($F(1.370, 9.592) = 1.214$, $P = 0.318$), though there was a trend for increased stepping errors after 4 and 23 days compared to baseline. In the hM3Dq

group, statistical analysis revealed significant differences in stepping errors across time points ($F(1.963, 19.63) = 6.865$, $P = 0.006$). Post-hoc analysis showed a significant increase in stepping errors on day 4 compared to baseline ($P = 0.034$) and a significant decrease compared to day 23 ($P = 0.021$), indicating an initial motor deficit followed by improvement during the recovery period. Notably, no significant difference was observed between day 23 and baseline in the hM3Dq group ($P = 0.992$), suggesting a return to baseline performance and thus complete recovery by day 23. In the hM4Di group, statistical analysis showed no significant differences in stepping errors over time ($F(1.438, 8.627) = 1.742$, $P = 0.229$), although there was a trend for worse performance after stroke without recovery. On day 23, the number of stepping errors did not significantly differ between the EGFP, hM3Dq, and hM4Di groups (Brown-Forsythe ANOVA: $F(2, 16.18) = 1.161$, $P = 0.338$; Welch's ANOVA: $W(2, 11.94) = 1.365$, $P = 0.293$), indicating similar levels of motor performance across groups at this time point (**Figure 14F**). However, only the hM3Dq group returned to baseline performance by day 23 in the irregular ladder rung test, while no significant recovery improvements were seen in the EGFP and hM4Di groups. This suggests that the enhanced serotonergic transmission in the DRN facilitated motor recovery following the stroke.

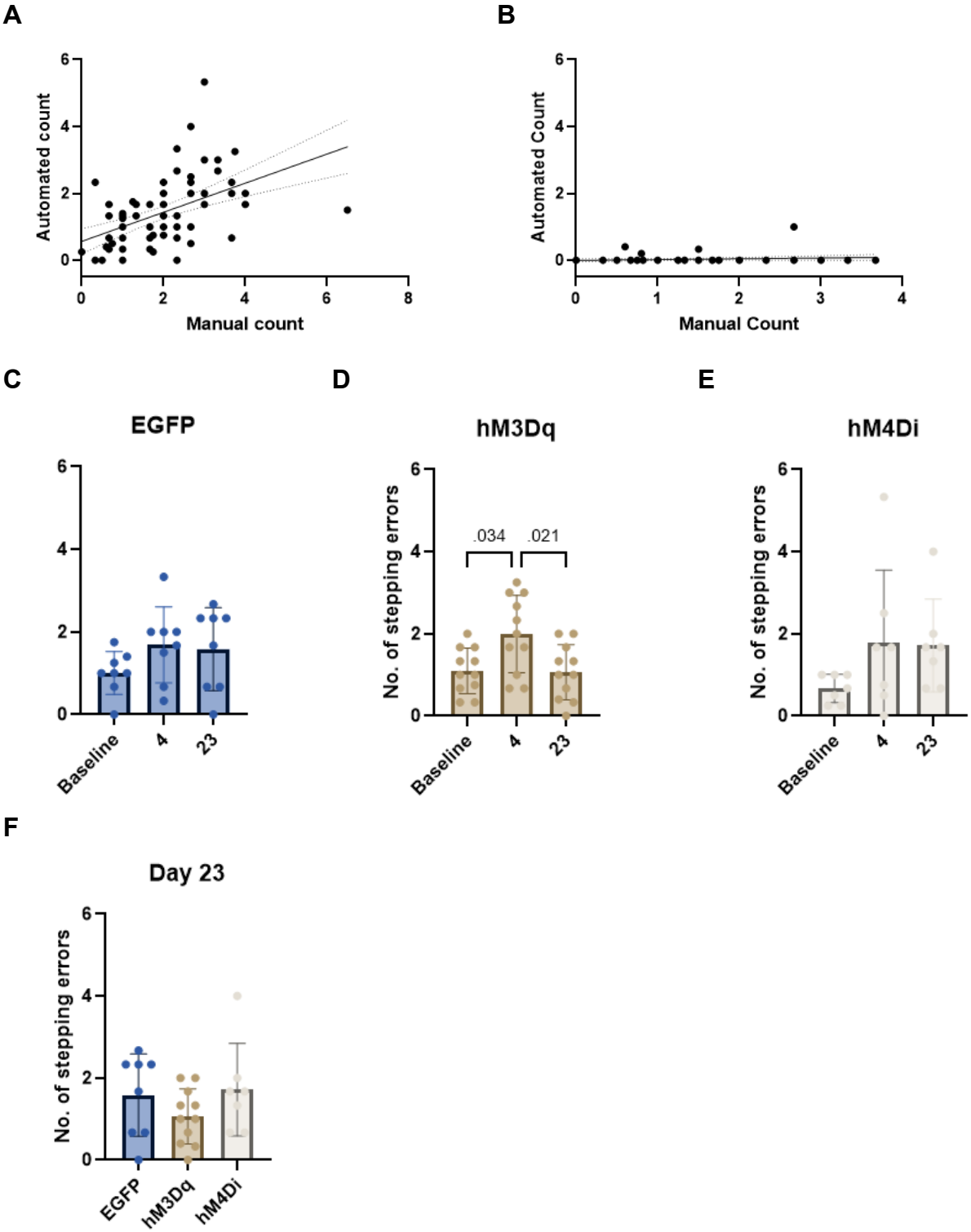

Figure 14. DRN serotonergic transmission improves recovery after stroke in the hM3Dq group. **A.** Regression plot of manual count vs. automated count of the contralateral paw. Simple linear regression with 95 % CI: R^2 = 0.2575, Y = 0.4354X + 0.5637, *P* < 0.0001). **B.** Regression plot of manual count vs. automated count of the ipsilateral paw. Simple linear regression with 95 % CI: R^2 = 0.0246, Y = 0.02342X - 0.0024, *P* = 0.1700. **C.** Automatically counted stepping errors of the contralateral paw in the EGFP group. One-way repeated measures ANOVA: F(1.370, 9.592) = 1.214, *P* = 0.318. **D.** Automatically counted stepping errors of the contralateral paw in the hM3Dq group. One-way repeated measures ANOVA with Tukey's post-hoc test: F(1.963, 19.63) = 6.865, *P* = 0.006. **E.** Automatically counted stepping errors of the contralateral paw in the hM4Di group. One-way repeated measures ANOVA: F(1.438, 8.627) = 1.742, *P* = 0.229. **F.** Comparison of the number of pellets reached on day 23 between EGFP, hM3Dq and hM4Di group in contralateral paw**.** One-way ANOVA: F(2, 16.18) = 1.161, *P* = 0.338.

5 Discussion

With this study, we showed that serotonergic transmission in the DRN facilitates functional recovery after stroke. We developed a mouse model that enables the specific chemogenetical activation or inactivation of serotonergic neurons in the DRN. Beyond stroke research, this mouse model may be useful to better understand the complex DRN system in other diseases, such as depression or movement disorders.

The development of the mouse model enabled the selective modulation of serotonergic transmission in the DRN through DREADDs. AAV injections led to a distinct transduction of serotonergic neurons in the DRN. However, we only found a partial co-localization of the DREADDs to serotonin (5-HT) immunostaining. Since the immunohistochemical staining we performed detects serotonin directly, it may only label neurons with high concentrations of serotonin. As a result, our histological analysis of 5-HT may not have fully captured all serotonergic neuron populations within the DRN. Nevertheless, we confirmed that hM3Dq receptor activation led to increased neuronal activity, as demonstrated by significantly higher cFOS expression compared to the EGFP group. This validates that serotonergic neurons were effectively transduced with functional DREADDs. However, we observed variability in the exact location of receptor expression within the DRN across subjects. This may have impacted the experimental outcomes since different regions within the DRN are partly associated with distinct functions (Ren et al., 2018) and suggests that more precise targeting of specific DRN subregions is necessary to minimize variability. However, by expressing DREADDs under the control of the TPH2 promoter, we were able to selectively modulate serotonergic neurons, ensuring that any observed behavioral changes are directly linked to serotonergic transmission. With this system, we have the possibility to control the activity of serotonin neurons in the DRN for both short (hours) and long (weeks) timeframes, while other systems such as optogenetics rather is useful for controlling the activity of neurons for short periods (seconds or minutes) (Ren et al., 2018).

We further validated that the mouse model effectively enhances DRN serotonergic transmission by observing expected behavioral changes in the EPM and open field test following hM3Dq receptor activation. We demonstrated that activating the DRN via hM3Dq resulted in increased anxiety-like behavior in the EPM, indicated by significantly less time spent in the open arms compared to the EGFP control group.

This aligns with previous findings, which showed that increased serotonergic activity in the DRN enhances anxiety-related responses (Ren et al., 2018; Sena et al., 2003). Ren et al. (2018) reported that serotonergic neurons in the dorsal part of the DRN exhibit anxiogenic effects, while those in the ventral DRN are associated with anxiolytic effects. This suggests that we primarily targeted the dorsal region of the DRN in our study.

In the open field test, the hM3Dq group showed a significant reduction in distance traveled compared to the EGFP group, suggesting that the activation of the hM3Dq receptor suppresses locomotor activity. This is consistent with studies showing that elevated DRN serotonergic transmission reduces locomotor activity (Ren et al., 2018).

In our study, we performed a dose-finding approach assessed with distance travelled in the open field as primary outcome measure to determine the optimal CNO dose for the activation of DREADDs while minimizing potential side effects. Jendryka et al. (2019) evaluated if CNO binds to other targets than the intended DREADDs and showed CNO also interacts with several other receptors, particularly the α1A adrenergic, H1 histamine, M1 muscarinic, and 5-HT2A/5-HT2B serotonin receptors. This highlights the potential for off-target effects when using CNO in experiments. Since we did not see a further reduction in distance travelled in the open field in the hM3Dq group at 1.0 mg/kg body weight compared to 0.5 mg/kg body weight, we suggest a ceiling effect at this dosage. To avoid unspecific behavioral effects and maximize intended effects of DREADD activation, we decided to use a dosage of 0.5 mg/kg body weight CNO in our experiment.

The hM4Di group, intended to reduce activity, showed no significant difference compared to EGFP. Moreover, we found no effect on behavioral outcomes in the EPM and the open field test in our study. This may be explained by the fact that we used 0.5 mg/kg body weight of CNO for hM4Di activation, whereas dose ranges of 3-5 mg/kg are typically considered effective for activating hM4Di in mice *in vivo* (Jendryka et al., 2019). These results suggest that 0.5 mg/kg body weight is an effective dose for activating the DRN through the hM3Dq receptor, but insufficient for inhibiting activity via the hM4Di receptor. However, increasing the dose for hM4Di may have produced side effects, as seen with the 1.0 mg/kg dose in the EGFP group, where slightly reduced locomotor activity in the open field was observed compared to 0.5 mg/kg body weight. This reduction could be attributed to the metabolism of CNO to clozapine,

which has been shown in previous studies to influence behavioral outcomes (MacLaren et al., 2016). This would have potentially biased the interpretation of the results by confounding the effects of the treatment. We therefore demonstrated that we were able to successfully develop a mouse model that selectively modulates serotonergic transmission in the DRN using DREADDs at a CNO dosage of 0.5 mg/kg body weight, avoiding side-effects by CNO.

We found that enhancing DRN serotonergic transmission promotes recovery following stroke. This effect was observed in the irregular ladder rung test, which assesses both skilled walking and coordination (Metz & Whishaw, 2009), but not in the staircase task, which primarily evaluates skilled reaching (Baird et al., 2001). The performance in the irregular ladder rung test returned to baseline in the hM3Dq group, suggesting effective functional recovery, potentially due to enhanced neuroplasticity or compensatory mechanisms. This aligns with the findings from Ng et al. (2015), who demonstrated that fluoxetine can prolong the window for recovery of upper limb function after stroke by enhancing neuroplasticity even when motor training is delayed. The lack of significant differences in stepping errors in the irregular ladder rung between the groups on day 23 may be attributed to factors such as the small sample size and the complexity of the underlying experimental system. The variability in the location of the DREADD expression across subjects could have contributed to a reduced effect size, since it could have affected overall recovery outcomes. However, since the hM3Dq group completely recovered whereas the EGFP and hM4Di group showed a persistent deficit, these results indicate that enhancing DRN serotonergic transmission promoted recovery after stroke, particularly in tasks requiring skilled walking and coordination, such as the irregular ladder rung test. This indicates that increased DRN serotonergic transmission enhanced reorganization and adaptation of the brain after stroke, leading to functional improvements over time.

The improvement through DRN serotonergic transmission may be specific to certain motor skills, such as balance and coordination, which are tested more pronounced in the irregular ladder rung test. The staircase task, focusing on repetitive forelimb reaching movements, may not reflect the same motor improvements as the ladder rung test. Moreover, our endpoint measure in the staircase task did not distinguish between movement patterns. To better assess recovery, advanced kinematic analysis could offer a more comprehensive understanding of post-stroke movement dynamics.

Skrobot et al. (2024) demonstrated that advanced kinematic analysis revealed post-stroke deficits in slips and reach events, while traditional pellet counting failed to detect any differences. This underscores the limitations of basic measures and the need for more detailed movement analysis to detect subtle differences in recovery. It also highlights the variability between behavioral tests, showing that some may be more sensitive to specific aspects of motor recovery than others, further emphasizing the importance of selecting appropriate tasks or doing multiples behavior tests when evaluating functional outcomes after stroke.

Serotonin plays a critical role in regulating plasticity, including sprouting and synaptogenesis (Mattson et al., 2004; Vahid-Ansari et al., 2019), processes that are also associated with recovery after stroke (Teasell et al., 2005). The FLAME and FOCUS trials provide valuable clinical context for discussing the role of serotonergic modulation in stroke recovery. The FLAME trial showed that the selective serotonin reuptake inhibitor fluoxetine enhanced motor recovery in patients with ischemic stroke after 3 months (Chollet et al., 2011). This aligns with our findings where enhancing DRN serotonergic transmission promoted functional recovery, particularly in tasks involving balance and coordination, as seen in the irregular ladder rung test. On the other hand, the FOCUS trial, which observed no significant improvement in functional outcomes at 6 months, underscores the complexity of fluoxetine's systemic effects (Dennis et al., 2019).

However, it is important to note that the two clinical trials differ in their outcome measures and the time points at which those outcomes were assessed. The FLAME trial focused on motor recovery over 3 months using the Fugl-Meyer Motor Score, while the FOCUS trial extended the observation period to 6 months and primarily assessed functional outcomes with the modified Rankin Scale. In both trials 20 mg fluoxetine were administered daily and the treatment started in the early post-stroke period. Moreover, while all patients in the FLAME study underwent rehabilitation therapies, the FOCUS trial did not require patients to participate in rehabilitative therapies. However, it should be emphasized that neither in the FLAME trial nor in the FOCUS trial, the physical therapy regimens were standardized by the trial protocols and were instead regulated by the individual participating centers. Therefore, there may have been variability in the intensity and quality of the physical therapy that patients received, which could have contributed to differences in outcomes of both studies.

In contrast to the FLAME and FOCUS study, in which a global induction of serotonergic systems in the brain by fluoxetine was examined, we specifically targeted the serotonergic neurons of the DRN through DREADD activation. By this, we provided insights into the function of a specific serotonergic system. We showed that the serotonergic DRN system is sufficient to improve motor recovery, particularly in skills requiring coordination, suggesting that enhancing serotonergic transmission in specific brain circuits could be a more effective therapeutic strategy than systemic treatments. Therefore, while clinical studies with the systemically acting SSRI fluoxetine provide contradicting results, targeting DRN activation may provide more precise and consistent improvements, thereby offering promising therapeutic approaches for enhancing post-stroke recovery through neuromodulation strategies.

5.1 Limitations of the study

In this study, we decided to use the photothrombotic stroke model because it allows precise control over the location and size of the stroke, ensuring uniform lesion volumes in the motor cortex. Since viral DREADD injections can introduce variability in experimental outcomes, this stroke model was helpful for maintaining consistency in stroke induction, minimizing additional variability, and allowing clearer interpretation of the results. However, unlike human ischemic strokes, the photothrombotic model does not produce an ischemic penumbra, a partially ischemic tissue region surrounding the core infarct where timely medical intervention can potentially restore function and prevent further injury (Labat-gest & Tomasi, 2013). We will continue further studies using stroke models that better mimic the pathophysiology of human stroke to provide a more realistic environment to study the effects of DRN serotonergic transmission on motor recovery after stroke.

Additionally, one limitation of this study is the lack of validation for the 5-HT antibody that we used. We were unable to validate the antibody ourselves and could not find any published studies confirming its validation. Since the antibody detects serotonin directly, it may only label neurons with high concentrations of serotonin and our histological analysis may not have fully captured all serotonergic neuron populations within the DRN. Future studies should include proper antibody validation to ensure the reliability of these findings.

Another limitation of this study is the inconsistency in the location of viral expression across the animals. While efforts were made to target the same brain region in each animal, slight variations in injection site or diffusion of the virus could have led to differences in the extent and location of DREADD expression. This inconsistency could introduce variability in the behavioral outcomes.

Further, this study had a relatively small sample size, which may have reduced the statistical power to detect subtle or less pronounced effects. Future studies with a larger sample size could reduce the variability between subjects, leading to more robust conclusions. Additionally, future studies should aim to refine targeting methods or consider using alternative approaches to achieve more precise and consistent viral expression across subjects.

6 Conclusion and outlook

Motor recovery after stroke remains challenging, as many patients do not achieve full recovery and continue to experience long-term impairments despite rehabilitation efforts. Our study demonstrated that enhancing DRN serotonergic transmission can promote motor recovery following stroke in a photothrombotic mouse model.

We successfully developed a mouse model that specifically activates DRN serotonergic transmission and validated it by demonstrating that this activation resulted in reduced locomotion and heightened anxiety-related behavior, as this phenotype is documented in the literature for increased DRN serotonergic transmission (Ren et al., 2018; Sena et al., 2003). Moreover, the phenotype observed in the hM3Dq group was accompanied by increased expression of the neuronal activity marker cFOS, indicating heightened neuronal activity in response to DREADD activation. In contrast, the inhibition of serotonergic transmission via the hM4Di receptor did not produce a distinct phenotype compared to the control group at any dosage tested. We therefore identified a CNO dosage of 0.5 mg/kg body weight as optimal for activating DRN serotonergic transmission, as higher doses resulted in side effects. However, this dosage may have been insufficient for effectively inhibiting DRN transmission in our mouse model.

Our findings demonstrated that activation of DRN serotonergic transmission significantly promoted motor recovery, particularly in tasks requiring coordination and skilled walking, as seen in the irregular ladder rung test. The effects on skilled reaching were less pronounced, highlighting the complexity of motor system and reorganization after stroke and the focus of different behavioral tests.

Unlike global SSRI treatments, which have shown mixed results in clinical trials such as the FLAME trial and FOCUS trial, selective modulation of the DRN could offer a more precise and effective therapeutic strategy for motor recovery. The targeted neuromodulation of DRN serotonergic neurons may improve recovery more efficiently than broad systemic treatments, providing a promising avenue for future therapeutic interventions in stroke rehabilitation.

In conclusion, this study provides new insights into the role of DRN serotonergic transmission in post-stroke recovery and underscores the therapeutic potential of targeting specific brain circuits to enhance neuroplasticity.

More advanced behavioral assessments of the staircase test may help identify subtle differences in movement dynamics between groups, which could further clarify the potential therapeutic role of serotonergic modulation in stroke recovery also in the context of skilled reaching and fine movement patterns. To further validate these findings and translate them into clinical relevance, future research should also employ stroke models that more closely mimic human stroke pathophysiology than photothrombosis by including an infarct core and a penumbra.

Additionally, functional MRI assessments could help clarify which brain networks are activated or inhibited during DRN modulation, providing deeper insights into how serotonergic transmission affects stroke recovery. This could be particularly helpful given the mixed results in the literature regarding the specific networks influenced by DRN activation (Grandjean et al., 2019; Hamada et al., 2024). Combining this with advanced behavioral assessments, such as tracking forepaw and hindpaw movements, could reveal motor recovery and compensatory mechanisms, enabling the correlation of movement dynamics with functional network changes and the effects of DRN modulation. This approach could provide deeper insights and help harness these mechanisms for improved stroke rehabilitation strategies. Several studies have explored neurostimulation techniques, such as transcranial magnetic stimulation and deep brain stimulation in stroke recovery, which aim to modulate neuronal pathways and enhance task-specific plasticity in motor recovery following stroke (Dawson et al., 2024). Considering the ability of DRN serotonergic transmission to enhance plasticity in motor recovery, targeted DRN stimulation presents a promising avenue for future neurostimulation interventions in the context of motor recovery after stroke.

7 References

Bachmann, L. C., Lindau, N. T., Felder, P., & Schwab, M. E. (2014). Sprouting of Brainstem–Spinal Tracts in Response to Unilateral Motor Cortex Stroke in Mice. The Journal of Neuroscience, 34(9), 3378–3389. https://doi.org/10.1523/JNEUROSCI.4384-13.2014

Bacqué-Cazenave, J., Bharatiya, R., Barrière, G., Delbecque, J.-P., Bouguiyoud, N., Di Giovanni, G., Cattaert, D., & De Deurwaerdère, P. (2020). Serotonin in Animal Cognition and Behavior. International Journal of Molecular Sciences, 21(5), Article 5. https://doi.org/10.3390/ijms21051649

Baird, A. L., Meldrum, A., & Dunnett, S. B. (2001). The staircase test of skilled reaching in mice. Brain Research Bulletin, 54(2), 243–250. https://doi.org/10.1016/S0361-9230(00)00457-3

Brott Thomas & Bogousslavsky Julien. (2000). Treatment of Acute Ischemic Stroke. New England Journal of Medicine, 343(10), 710–722. https://doi.org/10.1056/NEJM200009073431007

Chollet, F., Tardy, J., Albucher, J.-F., Thalamas, C., Berard, E., Lamy, C., Béjot, Y., Deltour, S., Jaillard, A., Niclot, P., Guillon, B., Moulin, T., Marque, P., Pariente, J., Arnaud, C., & Loubinoux, I. (2011). Fluoxetine for motor recovery after acute ischaemic stroke (FLAME): A randomised placebo-controlled trial. Lancet neurology, 10, 123–130. https://doi.org/10.1016/S1474-4422(10)70314-8

Chung, L. (2015). A Brief Introduction to the Transduction of Neural Activity into Fos Signal. Development & Reproduction, 19(2), 61–67. https://doi.org/10.12717/DR.2015.19.2.061

Cohen-Cory, S., Kidane, A. H., Shirkey, N. J., & Marshak, S. (2010). Brain-derived neurotrophic factor and the development of structural neuronal connectivity. Developmental Neurobiology, 70(5), 271–288. https://doi.org/10.1002/dneu.20774

Commons, K. G. (2015). Two major network domains in the dorsal raphe nucleus. Journal of Comparative Neurology, 523(10), 1488–1504. https://doi.org/10.1002/cne.23748

Dawson, J., Abdul-Rahim, A. H., & Kimberley, T. J. (2024). Neurostimulation for treatment of post-stroke impairments. Nature Reviews Neurology, 20(5), 259–268. https://doi.org/10.1038/s41582-024-00953-z

Dennis, M., Mead, G., Forbes, J., Graham, C., Hackett, M., Hankey, G. J., House, A., Lewis, S., Lundström, E., Sandercock, P., Innes, K., Williams, C., Drever, J., Mcgrath,

A., Deary, A., Fraser, R., Anderson, R., Walker, P., Perry, D., … Hungwe, R. (2019). Effects of fluoxetine on functional outcomes after acute stroke (FOCUS): A pragmatic, double-blind, randomised, controlled trial. The Lancet, 393(10168), 265–274. https://doi.org/10.1016/S0140-6736(18)32823-X

Feigin, V. L., Stark, B. A., Johnson, C. O., Roth, G. A., Bisignano, C., Abady, G. G., Abbasifard, M., Abbasi-Kangevari, M., Abd-Allah, F., Abedi, V., Abualhasan, A., Abu-Rmeileh, N. M., Abushouk, A. I., Adebayo, O. M., Agarwal, G., Agasthi, P., Ahinkorah, B. O., Ahmad, S., Ahmadi, S., … Murray, C. J. L. (2021). Global, regional, and national burden of stroke and its risk factors, 1990–2019: A systematic analysis for the Global Burden of Disease Study 2019. The Lancet Neurology, 20(10), 795–820. https://doi.org/10.1016/S1474-4422(21)00252-0

Feske, S. K. (2021). Ischemic Stroke. The American Journal of Medicine, 134(12), 1457–1464. https://doi.org/10.1016/j.amjmed.2021.07.027

Grandjean, J., Corcoba, A., Kahn, M. C., Upton, A. L., Deneris, E. S., Seifritz, E., Helmchen, F., Mansuy, I. M., Mann, E. O., Rudin, M., & Saab, B. J. (2019). A brain-wide functional map of the serotonergic responses toacute stress and fluoxetine. Nature Communications, 10(1), 350. https://doi.org/10.1038/s41467-018-08256-w

Hamada, H. T., Abe, Y., Takata, N., Taira, M., Tanaka, K. F., & Doya, K. (2024). Optogenetic activation of dorsal raphe serotonin neurons induces brain-wide activation. Nature Communications, 15(1), 4152. https://doi.org/10.1038/s41467-024-48489-6

Hermann, D. M., & Chopp, M. (2012). Promoting brain remodelling and plasticity for stroke recovery: Therapeutic promise and potential pitfalls of clinical translation. The Lancet Neurology, 11(4), 369–380. https://doi.org/10.1016/S1474-4422(12)70039-X

Hornung, J.-P. (2003). The human raphe nuclei and the serotonergic system. Journal of Chemical Neuroanatomy, 26(4), 331–343. https://doi.org/10.1016/j.jchemneu.2003.10.002

Huang, K. W., Ochandarena, N. E., Philson, A. C., Hyun, M., Birnbaum, J. E., Cicconet, M., & Sabatini, B. L. (2019). Molecular and anatomical organization of the dorsal raphe nucleus. eLife, 8, e46464. https://doi.org/10.7554/eLife.46464

Hudson, A. E. (2018). Chapter Twelve - Genetic Reporters of Neuronal Activity: C-Fos and G-CaMP6. In R. G. Eckenhoff & I. J. Dmochowski (Hrsg.), Methods in Enzymology (Bd. 603, S. 197–220). Academic Press. https://doi.org/10.1016/bs.mie.2018.01.023

Jendryka, M., Palchaudhuri, M., Ursu, D., Van Der Veen, B., Liss, B., Kätzel, D.,

Nissen, W., & Pekcec, A. (2019). Pharmacokinetic and pharmacodynamic actions of clozapine-N-oxide, clozapine, and compound 21 in DREADD-based chemogenetics in mice. Scientific Reports, 9(1), 4522. https://doi.org/10.1038/s41598-019-41088-2

Jiang, L., Xu, H., & Yu, C. (2013). Brain Connectivity Plasticity in the Motor Network after Ischemic Stroke. Neural Plasticity, 2013(1), 924192. https://doi.org/10.1155/2013/924192

Kalueff, A. V., Fox, M. A., Gallagher, P. S., & Murphy, D. L. (2007). Hypolocomotion, anxiety and serotonin syndrome-like behavior contribute to the complex phenotype of serotonin transporter knockout mice. Genes, Brain and Behavior, 6(4), 389–400. https://doi.org/10.1111/j.1601-183X.2006.00270.x

Knab, F., Koch, S. P., Major, S., Farr, T. D., Mueller, S., Euskirchen, P., Eggers, M., Kuffner, M. T. C., Walter, J., Berchtold, D., Knauss, S., Dreier, J. P., Meisel, A., Endres, M., Dirnagl, U., Wenger, N., Hoffmann, C. J., Boehm-Sturm, P., & Harms, C. (2023). Prediction of Stroke Outcome in Mice Based on Noninvasive MRI and Behavioral Testing. Stroke, 54(11), 2895–2905. https://doi.org/10.1161/STROKEAHA.123.043897

Koch, S., Mueller, S., Foddis, M., Bienert, T., von Elverfeldt, D., Knab, F., Farr, T. D., Bernard, R., Dopatka, M., Rex, A., Dirnagl, U., Harms, C., & Boehm-Sturm, P. (2019). Atlas registration for edema-corrected MRI lesion volume in mouse stroke models. Journal of Cerebral Blood Flow & Metabolism, 39(2), 313–323. https://doi.org/10.1177/0271678X17726635

Kuriakose, D., & Xiao, Z. (2020). Pathophysiology and Treatment of Stroke: Present Status and Future Perspectives. International Journal of Molecular Sciences, 21(20), Article 20. https://doi.org/10.3390/ijms21207609

Labat-gest, V., & Tomasi, S. (2013). Photothrombotic Ischemia: A Minimally Invasive and Reproducible Photochemical Cortical Lesion Model for Mouse Stroke Studies. Journal of Visualized Experiments : JoVE, 76, 50370. https://doi.org/10.3791/50370

Li, S. (2017). Spasticity, Motor Recovery, and Neural Plasticity after Stroke. Frontiers in Neurology, 8. https://doi.org/10.3389/fneur.2017.00120

Manvich, D. F., Webster, K. A., Foster, S. L., Farrell, M. S., Ritchie, J. C., Porter, J. H., & Weinshenker, D. (2018). The DREADD agonist clozapine N-oxide (CNO) is reverse-metabolized to clozapine and produces clozapine-like interoceptive stimulus effects in rats and mice. Scientific Reports, 8(1), 3840. https://doi.org/10.1038/s41598-018-22116-z

Martinowich, K., & Lu, B. (2008). Interaction between BDNF and Serotonin: Role in Mood Disorders. Neuropsychopharmacology, 33(1), 73–83. https://doi.org/10.1038/sj.npp.1301571

Mathis, A., Mamidanna, P., Cury, K. M., Abe, T., Murthy, V. N., Mathis, M. W., & Bethge, M. (2018). DeepLabCut: Markerless pose estimation of user-defined body parts with deep learning. Nature Neuroscience, 21(9), 1281–1289. https://doi.org/10.1038/s41593-018-0209-y

Mattson, M. P., Maudsley, S., & Martin, B. (2004). BDNF and 5-HT: A dynamic duo in age-related neuronal plasticity and neurodegenerative disorders. Trends in Neurosciences, 27(10), 589–594. https://doi.org/10.1016/j.tins.2004.08.001

Metz, G. A., & Whishaw, I. Q. (2009). The Ladder Rung Walking Task: A Scoring System and its Practical Application. Journal of Visualized Experiments : JoVE, 28, 1204. https://doi.org/10.3791/1204

Michelsen, K. A., Prickaerts, J., & Steinbusch, H. W. M. (2008). The dorsal raphe nucleus and serotonin: Implications for neuroplasticity linked to major depression and Alzheimer's disease. In G. Di Giovann, V. Di Matteo, & E. Esposito (Hrsg.), Progress in Brain Research (Bd. 172, S. 233–264). Elsevier. https://doi.org/10.1016/S0079-6123(08)00912-6

Murphy, T. H., & Corbett, D. (2009). Plasticity during stroke recovery: From synapse to behaviour. Nature Reviews Neuroscience, 10(12), Article 12. https://doi.org/10.1038/nrn2735

Musumeci, G., Loreto, C., Trovato, F. M., Giunta, S., Imbesi, R., & Castrogiovanni, P. (2014). Serotonin (5HT) expression in rat pups treated with high-tryptophan diet during fetal and early postnatal development. Acta Histochemica, 116(2), 335–343. https://doi.org/10.1016/j.acthis.2013.08.011

Ng, K. L., Gibson, E. M., Hubbard, R., Yang, J., Caffo, B., O'Brien, R. J., Krakauer, J. W., & Zeiler, S. R. (2015). Fluoxetine Maintains a State of Heightened Responsiveness to Motor Training Early After Stroke in a Mouse Model. Stroke, 46(10), 2951–2960. https://doi.org/10.1161/STROKEAHA.115.010471

Okaty, B. W., Commons, K. G., & Dymecki, S. M. (2019). Embracing diversity in the 5-HT neuronal system. Nature Reviews Neuroscience, 20(7), 397–424. https://doi.org/10.1038/s41583-019-0151-3

Okaty, B. W., Sturrock, N., Escobedo Lozoya, Y., Chang, Y., Senft, R. A., Lyon, K. A., Alekseyenko, O. V., & Dymecki, S. M. (2020). A single-cell transcriptomic and anatomic

atlas of mouse dorsal raphe Pet1 neurons. eLife, 9, e55523. https://doi.org/10.7554/eLife.55523

Ollivier, M., Soto, J. S., Linker, K. E., Moye, S. L., Jami-Alahmadi, Y., Jones, A. E., Divakaruni, A. S., Kawaguchi, R., Wohlschlegel, J. A., & Khakh, B. S. (2024). Crym-positive striatal astrocytes gate perseverative behaviour. Nature, 627(8003), 358–366. https://doi.org/10.1038/s41586-024-07138-0

Phipps, M. S., & Cronin, C. A. (2020). Management of acute ischemic stroke. Bmj, 368. https://www.bmj.com/content/368/bmj.l6983.short

Ren, J., Friedmann, D., Xiong, J., Liu, C. D., Ferguson, B. R., Weerakkody, T., DeLoach, K. E., Ran, C., Pun, A., Sun, Y., Weissbourd, B., Neve, R. L., Huguenard, J., Horowitz, M. A., & Luo, L. (2018). Anatomically Defined and Functionally Distinct Dorsal Raphe Serotonin Sub-systems. Cell, 175(2), 472-487.e20. https://doi.org/10.1016/j.cell.2018.07.043

Roth, B. L. (2016). DREADDs for Neuroscientists. Neuron, 89(4), 683–694. https://doi.org/10.1016/j.neuron.2016.01.040

Schneider, C. L., Majewska, A. K., Busza, A., Williams, Z. R., Mahon, B. Z., & Sahin, B. (2021). Selective serotonin reuptake inhibitors for functional recovery after stroke: Similarities with the critical period and the role of experience-dependent plasticity. Journal of Neurology, 268(4), 1203–1209. https://doi.org/10.1007/s00415-019-09480-0

Sena, L. M., Bueno, C., Pobbe, R. L. H., Andrade, T. G. C. S., Zangrossi, H., & Viana, M. B. (2003). The dorsal raphe nucleus exerts opposed control on generalized anxiety and panic-related defensive responses in rats. Behavioural Brain Research, 142(1), 125–133. https://doi.org/10.1016/S0166-4328(02)00399-6

Skrobot, M., Sa, R. D., Walter, J., Vogt, A., Paulat, R., Lips, J., Mosch, L., Mueller, S., Dominiak, S., Sachdev, R., Boehm-Sturm, P., Dirnagl, U., Endres, M., Harms, C., & Wenger, N. (2024). Refined movement analysis in the Staircase test reveals differential motor deficits in mouse models of stroke. Journal of Cerebral Blood Flow & Metabolism, 0271678X241254718. https://doi.org/10.1177/0271678X241254718

Sternson, S. M., & Roth, B. L. (2014). Chemogenetic Tools to Interrogate Brain Functions. Annual Review of Neuroscience, 37(1), 387–407. https://doi.org/10.1146/annurev-neuro-071013-014048

Tatem, K. S., Quinn, J. L., Phadke, A., Yu, Q., Gordish-Dressman, H., & Nagaraju, K. (2014). Behavioral and Locomotor Measurements Using an Open Field Activity

Monitoring System for Skeletal Muscle Diseases. Journal of Visualized Experiments : JoVE, 91, 51785. https://doi.org/10.3791/51785

Teasell, R., Bayona, N. A., & Bitensky, J. (2005). Plasticity and Reorganization of the Brain Post Stroke. Topics in Stroke Rehabilitation, 12(3), 11–26. https://doi.org/10.1310/6AUM-ETYW-Q8XV-8XAC

Tennant, K. A., Adkins, D. L., Donlan, N. A., Asay, A. L., Thomas, N., Kleim, J. A., & Jones, T. A. (2011). The Organization of the Forelimb Representation of the C57BL/6 Mouse Motor Cortex as Defined by Intracortical Microstimulation and Cytoarchitecture. Cerebral Cortex, 21(4), 865–876. https://doi.org/10.1093/cercor/bhq159

Vahid-Ansari, F., Zhang, M., Zahrai, A., & Albert, P. R. (2019). Overcoming Resistance to Selective Serotonin Reuptake Inhibitors: Targeting Serotonin, Serotonin-1A Receptors and Adult Neuroplasticity. Frontiers in Neuroscience, 13. https://doi.org/10.3389/fnins.2019.00404

Walf, A. A., & Frye, C. A. (2007). The use of the elevated plus maze as an assay of anxiety-related behavior in rodents. Nature protocols, 2(2), 322–328. https://doi.org/10.1038/nprot.2007.44

Weber, R. Z., Mulders, G., Kaiser, J., Tackenberg, C., & Rust, R. (2022). Deep learning-based behavioral profiling of rodent stroke recovery. BMC Biology, 20(1), 232. https://doi.org/10.1186/s12915-022-01434-9

Zhu, H., Aryal, D. K., Olsen, R. H. J., Urban, D. J., Swearingen, A., Forbes, S., Roth, B. L., & Hochgeschwender, U. (2016). Cre-dependent DREADD (Designer Receptors Exclusively Activated by Designer Drugs) mice. Genesis, 54(8), 439–446. https://doi.org/10.1002/dvg.22949